Dear Editor, dear Reviewer,

the authors wish to thank again the reviewer for the detailed review containing many helpful remarks and constructive criticism.

From the review below we have identified, that you have still these major concerns:

1) validation of SMB forcing

2) the modified RCP2.6 scenario without overshoot

3) reference times for SMB forcing and temperature time series

As these concerns appear at several locations in the review, we will answer to them at one place marked with “Answer to MC1,2,3,”. At the other locations, we will refer to this comment.

We think, that our wording to refer to GCM’s also when we present and discuss output of SEMIC driven by GCMs might have lead to serious confusion for which we apologize. In order to distinguish better in the current version, we have introduced e.g. SEMIC-HadGEM in order to denote the resulting fields from SEMIC. We hope that this helps to dissolve this issue for future readers.

Further technicalities: below we answer each point raised by the reviewer and mark our answer in green colour. Our point-to-point answers to the previews review and where kept by the reviewer and also parts of the first reviews are included, so we kept them here too. Every text from a previous review is in italic, either reviewers in black or our response in blue. ‘Done.' denotes that this point is solved in the revised version of the manuscript. This could be that it will be either done directly, or that due to other changes the point does not arise any more, or that the point has been answered at another place in this text already.

We recognise that our manuscript is/was very labour intensive to review and we want to thank sincerely reviewer 1 and the editor for all the time and effort spent to improve the manuscript. In the course of revising the manuscript we spend a lot of time discussing the view of climate modellers on our way of dealing with GCM output, as well as ice flow modellers perspective of forcing ice models. We can say that we learnt a lot from these discussions, which only appeared due to the critics raised in the review. Many thanks!

Best wishes,

Martin & Co-authors

Reviewer 1

Summary

I am evaluating this paper for the second time after major revisions in the first round. The manuscript has changed considerably since the last iteration, has improved in response to the reviewer's comments and has seen new material being added. However, some major issues remain or have been introduced with the modifications, as is the case for the validation part and the “scenarios without overshoot”. The language also needs further improvements to clean up errors and make the text clearer.

I will first respond to some of the author comments (blue), with my initial comments indented twice. General and specific comments on the new version follow below.

Response to the discussion

Yes, indeed this is an important point and we followed the reviewers suggestion. With using the parameters of Krapp et al. (2017) the direct output of the SMB from SEMIC has a misfit of about ~2m/a and a correlation of ~r^2=0.5 by comparing SMB_RACMO_1960-1990 and dSMB_SEMIC_1960-1990 (almost similar for all GCMs used).

This evaluation should be extended and backed with figures to appear also in the manuscript. See general comments.

See answer MC1.

However, recalling Equation 3 and 4 from the manuscript, we do not use the direct output of SEMIC, but apply anomalies computed using SEMIC. The benefit of our approach is, that only the GCM trends of SMB changes are added to the RACMO SMB reference field, which represents the real SMB distribution very well. If we compare the computed SMB to RACMO (according to Eq. 3 and 4 without the synthetic SMBcorr), for instance for the HadGEM2-ES year 1990, it shows a very good agreement (Figure 2). See also answer to specific comment “p10 l2” below. In the revised manuscript we dedicate an own section to this issue.

This comparison does not really validate the SEMIC model. It only shows that at a given point (year 1990) the anomalies of SEMIC are close to zero. See general comments.

See answer MC1.

We expand the section about the SEMIC model in order to give the reader a better understanding of the model. In the new version of the manuscript we also review in the introduction section briefly the already existing alternatives used and relate the discussion section accordingly. The reason we have not included too much detail on that issue previously is, that we basically apply SEMIC and that the model in itself and all the parameter tuning is work done by Krapp et al., 2017. The advantage of using a semi-complexity model is indeed its simplicity and cost efficiency, which would allow ice sheet modellers to also run computation up to time scales of thousands of years (e.g. until 5000) studying long-term commitment of various emission scenarios and hence not be limited by the availability of regional climate model output.

Multi-millennial simulations are not relevant for the current study. The question is if the chosen model is an appropriate tool for the presented type of simulation. The SEMIC model has so far not been validated for the use with GCM input data, the way you are using it for the projections. Showing a proper validation is the price you have to pay for that novelty.

See answer MC1.

The authors rely on the parameter settings of the SEMIC model, which have been optimised for a different climate model input (Krapp et al., 2017). The Krapp et al. study shows that the SEMIC model can well approximate the MAR SMB results given MAR climate input. It must however be expected that the parameters that were chosen for a completely different climate input (different model, RCM vs GCM) are not optimal. Unless evidence can be provided that the applied parameters are indeed suited for the GCM forcing used in the present study, the model parameters should be optimised. Discussion on differences to other results (e.g. as done compared to Fürst et al., 2015) hinges on the implied sensitivity of the SMB model, which is currently not possible to be judged.

We haven chosen the same parameters of SEMIC as Krapp et al., 2017, due to the following reason: the

parameter tuning procedure performed by Krapp et al., 2017 aimed to find a parameter set which gives a best fit between SMB and skin temperature Ts of SEMIC with only a limited number of processes and simpler parameterisations than a regional climate model with full complexity would derive. As a regional climate model is typically validated against reanalysis data and observations, the best match between SMB and Ts of SEMIC and regional climate model (in that case MAR) is the best way to represent the processes and their parameters in SEMIC. We see it thus as a tuning of the parameterisation of the processes. Once the process description in SEMIC is optimised, any type of input, either GCM or reanalysis data fields, will lead to the best possible SMB and Ts fields that SEMIC can produce. Still, the GCM will lack the best atmospheric fields over the ice sheet, as it is limited in resolution compared to a regional climate model. Given experiences we made from these three GCMs used in this study, which are all have different drawbacks, which would mean to have a tuning for each of them and this tuning would then make the whole benefit of having a semi-complexity model with low costs meaningless. Furthermore, it would basically mean to compensate far too low near surface temperatures with SEMIC parameters, which would offset the whole comparison of GCM forcing. Therefore, we have chosen a different approach: we compensate for this by using the SEMIC output only as an anomaly.

I understand the argument to avoid tuning the model for individual GCMs and I agree with the point on compensating errors in the GCM. Nevertheless, I think you will agree that if you were to tune SEMIC for another RCM (say RACMO or HIRHAM), you would end up with different parameters. I believe it is important to recognise that, even if you chose to do nothing about it and use the MAR based parameters.

Yes, we agree, tuning SEMIC with another RCM will likely change the parameters, but we can only speculate to which extent. We followed the reviewer's recommendation for the comment p6 l7. Also, we added to the paragraph 2.2 (p6 l7): "If SEMIC is tuned with another RCM (e.g. RACMO or HIRHAM), the parameters will be different."

The situation here is worse, because using forcing from a GCM implies different characteristics, like smoother gradients and less resolved geometry compared to the RCM. It is possible that these characteristic differences between RCM and GCM (not individual model bias) have an important impact on the modelled SMB. I believe it is your responsibility to show that the parameters that you are using are indeed appropriate for the given purpose. You should show how the absolute SMB looks like for the different GCMs and compare that to reconstructions and/or state-of-the-art RCM results.

I agree that using the anomaly method is a good choice, as it circumvents *some* of the biases in the absolute SMB products you are producing with SEMIC. Nevertheless, the reference SMB has an important impact on the results, because of feedbacks and non- linearities. I insist that you show the total SEMIC SMB somewhere (possibly in an appendix or supplement) so that the quality of the model can be judged.

See Answer to MC1.

p6 l18 Not clear what the shortcomings of the Krapp method to treat albedo were and neither how this has been improved for the present study. This requires some additional description. Extending on the last comment, changes to the albedo scheme likely also have an impact on the SMB and would lead to different tuning even for the same climate model input.

We agree with the reviewer. We expand the section about the SEMIC model. In order to be consistent with parameters provided by Krapp et al. (2017) we switched back to the albedo scheme used by Krapp et al. (2017) for the new simulations.

So the improvement in the albedo scheme was not a very important improvement? As pointed out before, consistency may already be violated just by using a different climate model. Therefore, the consistency argument does not hold very strong for me.
For the first version of the manuscript, the resulting albedo was more plausible by using our "improved" albedo scheme compared to the scheme used by Krapp et al. (2017). But this was only due to the application error (mentioned in the preamble of our response in the first round of the review).

*p9 l25 These gradients were found as best fit to SMB simulated by a specific RCM (MAR) at different elevations. Applying these in your setup may be better than nothing, but for a consistent picture, these should ideally be recalculated based on your own model setup(SEMIC). Maybe, if you can run SEMIC at different elevation, you could get a feeling for the implied differences. *At the very least this inconsistency*

should be recognised and discussed as a shortcoming.*

This would be an interesting study. But for our application we follow the same argumentation above to the major point "parameter tuning". The parameters found by Edwards et al. (2014) are the most physical reliable and additionally we don't want to have different parameters between the three GCMs.

I agree with the argument that having different parameters for the different GCMs is not desirable and I see that it would be extra work to recalculate them with SEMIC. I completely disagree with the notion that the gradients are "the most physical reliable". These calculations have since been made with other models (e.g. Noël et al., 2016) with clearly different results, which shows that these parameters are model dependent and not unique solutions. I iterate my minimum requirement to mention in the text that the gradients are based on a different model setup and not consistent with the climate forcing applied for the projections.

We agree that "most physical reliable" is misleading here. Also, the intended sentence about this issue doesn't make it into the revised version of the manuscript for which we apologize. Now, we have added: "This relationship was estimated from a set of MAR simulations in which the ice sheet surface elevation was altered. [...] Please note, that the employed relationship with their parameters may change using a setup from SEMIC."

p11 l32 I am wondering in how far a detailed analysis of individual glaciers is justified given that an important aspect of the forcing in form of interaction with the ocean and sub-glacial hydrology is missing. The comparison suggests that we could hope to get the behaviour of individual glaciers in line with observations, which I consider very unlikely given the steady-state initialisation, coarse GCM-based forcing and lack of important forcing mechanisms.

This is indeed a good point raised. It is certainly true, that important forcing mechanisms like the oceanic forcing and subglacial hydrology are missing in this study, however, representing the dynamics of a glacier in the narrow fjords of Greenland well or representing the large NEGIS well, is only achieved with sufficient grid resolution and physics in the model, which our model both fulfils. This is indeed assessed by comparing individual glacier drainage basins with observation, like the surface velocity field. We are concerned about the statement 'given the steady-state initialisation' – we do not perform a steady-state initialisation at all, in contrast, we perform a complex initialisation procedure with mixture between inversion and paleo-spin ups. This procedure has been the top procedure in an international benchmark assessing the ability of models to achieve a good initial state (Goelzer et al., 2018). The reviewer seems to have overlooked this substantial part of this study. The coarse GCM-based forcing is subsequently processed in SEMIC is improving the resolution and the anomaly forcing is making sure, that the SMB in individual glacier basins is in high resolution – so the glacier basins are forced on high resolution.

With steady-state initialisation I mean that the attempt is to bring the ice sheet to a steady state at 1960. The way this is done here, no transient dynamical processes are active at that point that arise from past climate forcing. In the absence of dedicated ocean forcing, the response in ice flow and outlet glaciers can only be based on SMB forcing from 1960 onwards (and possibly some unwanted model drift). I believe this is also what the second reviewer had in mind for his second general comment on the omitting of ice dynamics.

The dynamical processes of past climate forcing are included in the way that the ice flow model is forced with it, but within the spin-up and inversion sequences, not the full geometric evolution is allowed, as this is (for all ice models) leading to initial states that are far from present day geometry. The response to past climate forcing is included, but not to the extent that all ice modellers would like to include it. As we stated before, the projections are based on SMB forcing, as the ocean forcing is kept fixed. This is, however, clearly stated in the manuscript and is also not such uncommon in ice flow model projection studies.

The claim to have the "top" procedure in the initMIP benchmark calls for some clarification. The model clearly achieves a very good match with the observed geometry. However, this is not the only factor that should be evaluated to judge the quality of an initialisation. It is specifically pointed out in the Goelzer et al. study that for this class of models, a better match with the observed geometry can be achieved by accepting a larger drift in the control experiment. The model drift in the control experiment of ISSM-AWI is the *largest* in the group of models with a similar initialisation method (data assimilation). Taking isolated results of an intercomparison out of context to falsely claim a superior modelling approach is

inappropriate and should be avoided.

With “top procedure” we refer here to a method that brings both initialization methods together: Long interglacial temperature spin-up and data-inversion. It should not be understand as the method of choice. And indeed, the drift is larger compared to similar initialization methods (inversion). But some of these models (e.g. JPL-ISSM) perform a relaxation run that is much larger than for the AWI-ISSM model (50.000 years compared to 50 years, respectively). For those models it is expected, that the drift is lower.

General comments

The validation presented in section 2.3 has important problems:

The correlation analysis shown in Figure 4 is not a meaningful validation. The year-to-year variability in the GCMs is not expected to coincided with that of RACMO, because the GCMs have their own internal variability. Correlation other than the long-term trend is pure coincidence, as can be seen from figure 3.

The comparison presented in Figure 5 is also meaningless, because the two SMB fields are by construction very similar. Panel a is RACMO(1990) and panel b is mean RACMO(1960-1990) + dSMB, where dSMB is by definition close to zero. The difference between the two is only due to inter-annual variability in RACMO and the GMCs, which again, are not expected to co-evolve.

In a first step, the absolute SMB of SEMIC for the different GCMs should be shown and compared to state-of-the-art RCM results.

Secondly, a meaningful validation of the SMB model in response to climate forcing is to force SEMIC with reanalysis data (e.g. ERA interim) and compare the resulting SMB with observations, RACMO or MAR. This is done for any other SMB model used for projections, whether in absolute mode or anomaly mode (e.g. Hanna et al., 2011, Fettweis et al., 2007, Noël et al., 2016, Vernon et al., 2013).

Afterwards it can be concluded that the absolute SMB is not ideal and the anomaly method can be applied.

Answer to MC1:

We are afraid that here a misunderstanding is arising. One thing is to validate the SMB model itself, meaning the way the energy balance is computed and the parameters that are tuned by Krapp et al. (2017). Another thing is to validate the SMB fields that are computed. A real validation is tricky, and is beyond the scope of this study. What we do instead is to assess how plausible the fields are. In this respect we compare them with RACMO in the same time period and check if both the pattern is matching reasonably and to check if the interannual variability is similar, meaning not exactly every year matching the total SMB, but to assess if years of extreme SMB are present in the SMB fields we have obtained using SEMIC and if the frequence matches reasonably with RACMO.

Additionally, we have forced SEMIC with ERA-Interim as requested and compare it with the absolute fields derived by SEMIC forced with the GCM data and RACMO2.3 (Figure below). Shown is a time average from 1979 to 2012. The spatial-integrated SMB for HadGEM2, IPSL, MIROC5, ERA-Interim and RACMO is 535, 556, 480, 143 and 351 Gt/a, respectively. Though the general large-scale patterns among all of these fields agree fairly well, there is an offset between the spatial-integrated SMB.

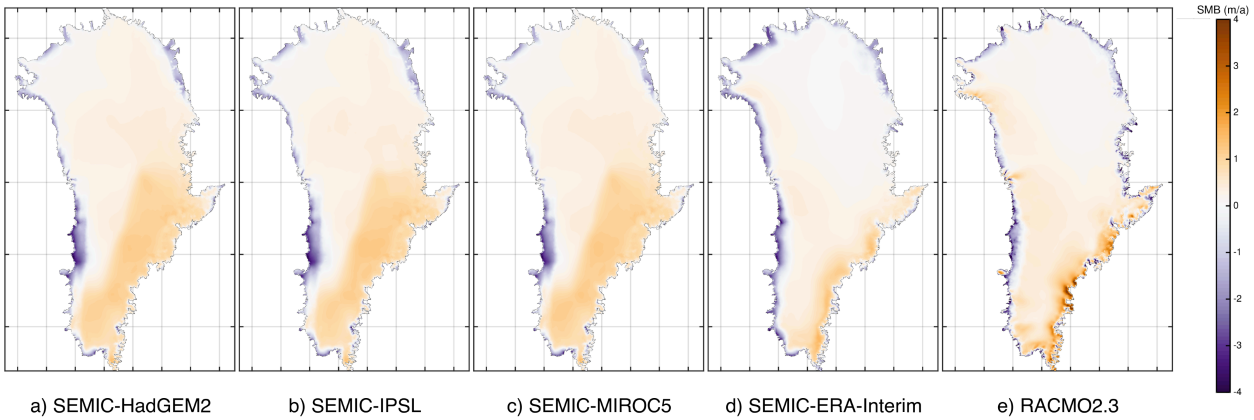

a) SEMIC-HadGEM2 b) SEMIC-IPSL c) SEMIC-MIROC5 d) SEMIC-ERA-Interim e) RACMO2.3

In order to assess the interannual variability, we show the time series from 1979-2012 of the spatial-averaged SMB for all of SMB fields (Figure below). The interannual variability is with respect to the frequency and magnitude in a good agreement. RACMO2.3 and ERA-Interim are basically coherent, which is not surprising as RACMO2.3 is forced with ERA-Interim.

We will present a comparison between RACMO and the absolute SMB field derived by forcing SEMIC with HadGEM2 for the reference time period of 1960-1990 (Fig. 3 in the new version of the manuscript).

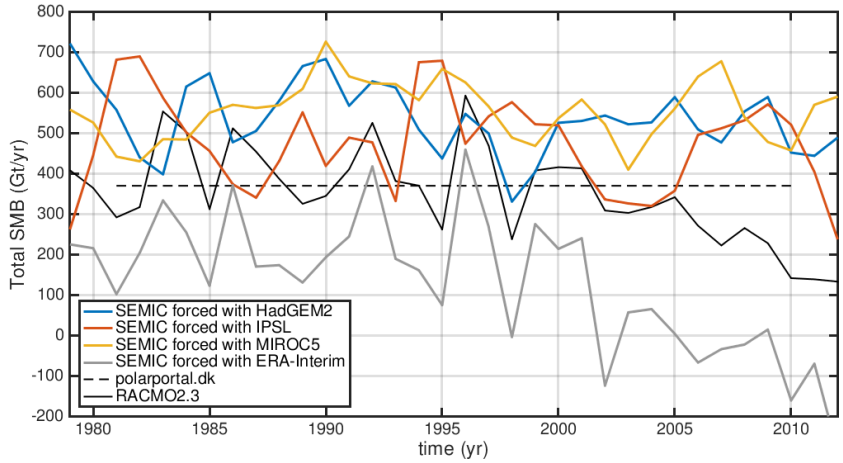

Additionally, a new figure of calculated variations between consecutive years demonstrates the interannual variability (Fig. 4 in the new version of the manuscript). Therefore, the old Figs. 4 and 5 in the manuscript are replaced by new figures.

The comparison we have made in the last version of the manuscript should not be understand as validating historical with reanalysis results. We intended to show, that our SMB forcing matches well the RACMO time series (as we thought this is what the reviewer requested). However, according to that, the choice of the year 1990 was not appropriate as ΔSMB is by definition small. However, replacing this exemplary 1990-analysis (Fig. 5) with the year 2016, the latest we have from the RACMO2.3 time, series where ΔSMB is not small, still shows a very good agreement (as you can see from the statistical values in Fig. 4). However, as mentioned above, this analysis is dropped in the new version of the manuscript and replaced by new figures.

A new "scenario" (without overshoot) has been added to the analysis. It is constructed by "cut-and-paste" based on the original RCP2.6 simulations of the individual GCMs. The procedure first identifies the time of overshoot for each individual GCM. Until this point the forcing remains the same as for the original scenario. From this point on an arbitrary 30 yr period from later in the individual simulations is repeated to

fill the length of the original simulation. I see a number of problems with this ad hoc approach that are mainly in relation to model dependency that complicates the comparison between the GCMs.

First, the resulting forcing time series should be shown. I suspect they will show a step change of the forcing at the moment of overshoot. I am not sure how to interpret such forcing as it is unphysical. It is also highly model dependent, I suppose the resulting forcing should not be called a scenario for that exact reason.

The choice of 30 year period seems arbitrary. Why not use instead e.g. the last 30 or 50 years of the simulation?. The strong multi-decadal variability visible in the SMB time series suggests that a much longer time period would be appropriate. How robust are results to a different choice of the period?

Answer to MC2:
We agree that the resulting forcing should be shown. The corresponding figure for the RCP2.6 scenario without overshoot is shown below. This figure is added to the new version of the manuscript as Fig. 5b.

There occurs no step change in the SMB time series. Indeed, the choice of the years from 2250-2280 is - to some extent - arbitrarily. The only restrictions that we made to the reused time period is a stabilized climate close to 1.5°C warming (in terms of temperature change, i.e. no long term decrease or increase in temperature) and to cover a time period with decadal variability to account for extreme years. Of course, we could use the last 30 or 50 years, but that will not change the results significantly. The frequency and amplitudes of the temperature change peaks (or increase/decrease of SMB) do not change too much. We have used different time periods of stagnant climate and the results (i.e. sea level contribution) are basically similar. In contrast, we have run the simulations with a reused time period around the “time of overshoot” where the warming still occurs. These simulations lead to more mass loss compared to the scenarios with overshoot. This also mentioned in the manuscript (p17 l12). This is due to the fact, that one would prolong the scenario with data of strongest climate change.

We have aimed to improve the description of the construction of this scenario in order to clarify the points raised in the review.

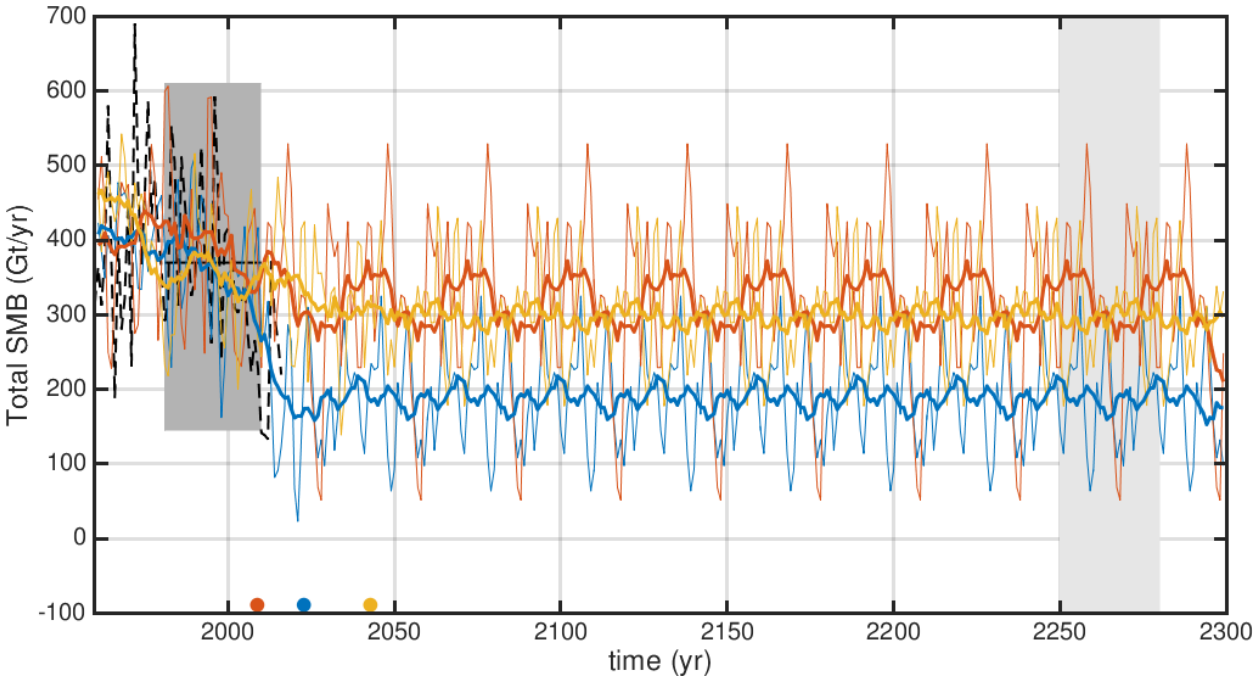

There may be a fundamental problem with the constructed time series because of using the anomaly method. The reference period for the SMB anomaly is 1960-1990, so the forcing is calculated relative to that period. The temperature time series used to diagnose the time of overshoot is referenced to another time period. This implies an offset of the forcing in function of the global temperature mismatch between the GCMs over the 1960-1990 reference period. I am not sure re-referencing will solve the problem

entirely, but it may be worth a try.

Answer to MC3:

First of all, we will not re-reference the temperature time series or re-analyze the diagnosed times of overshoot as the warming in the Paris Agreement is clearly defined as “warming above pre-industrial levels”. However, using a time period from 1960-1990 as the reference period for determining the time of overshoot will shift those for HadGEM2-ES from 2023 to 2024, for IPSL-CM5A-LR from 2009 to 2011 and for MIROC5 from 2043 to 2050. We think you will agree, that this will not change the SMB forcing for the constructed SMB for the RCP2.6 without overshoot dramatically. The shift is largest for MIROC5 but this is due to the fact that the warming is more gently and with that the decline in SMB.

The other way around, providing the SMB forcing relative to the same reference period as the temperature curve (Fig. 1) is unfeasible as the RACMO dataset is not available for the pre-industrial time period (1661-1880).

However, we think that the reference periods do not pose a major problem. The ΔSMB (Eq. 5) is per definition close to zero for the pre-industrial or the historical (approx. <1990) runs. So for any selected reference period (approx. <1990) we would end-up with more or less equal numbers for the reference SMBs from the GCMs and for the background SMB field (here SMB_RACMO(1960-1990)). Consequently - recall Eq. 4 - the course of the SMB forcing based on the original RCP2.6 scenario will not change but may be offset by a few Gt (but this would be buffered in the end by the imposed SMB_correction (Eq. 8)). The construction of the scenario without overshoot is therefore independent of the selected SMB reference period. The trends of the warming (Fig. 1) and the SMB forcing (Fig. 3) are therefore consistent and can be compared directly.

I am not sure addressing these points will be sufficient to make the taken approach look like a good idea. To revert to the original manuscript and removing the constructed forcing may be a viable option, too.

See answer to MC2 and MC3.

Specific comments

p1 l11 Clarify the use of scenarios in "for some scenarios". Probably you mean "for some models" or "for some experiments" if is any of the 3 models and 2 scenarios.

Done.

p1 l11-12 Why "most likely"? How do the different experiments differ in terms of the integrated SMB? Is there a clear difference between the runs that stabilise and those that continue to lose mass after 2300? Is SMB integrated in time or spatially? Clarify.

We dropped most likely. In the whole manuscript, integrated SMB refers to a spatially integrated SMB. In the revised version of the manuscript, we have added “spatial” or “time” where appropriate. The differences between spatial-integrated SMB can be seen in Fig. 3. None of the curves fall below zero (except for a few individual years).

p1 l14 Do you mean SEMIC or the GCMs in "stem from the underlying climate model"? Clarify.

Done. We mean GCM.

p1 l17 Delete "observed" after "observed"

Done

p2 l3-4 "mass loss" is caused by "acceleration" and decrease in SMB.

Done.

p2 l6 Maybe omit "regional" since the study is not concerned with it.

Done.

p2 l16 Also here, clarify the use of "other scenarios". See comment p1 l11.

Done.

p2 l19 place "has exceeded 1.5C ..." before "and may exceed 4C by 2100".

Done.

p2 l25 remove two times "very" before "scarce" and before "extensive".

Done.

p3 l6 Reformulate. "most suitable" may be true in some cases, but is certainly not generally true.

Done. We replaced “suitable” with “efficient”.

p3 l19 Replace "volume" by "thickness".

Done.

p3 l19 Remove "surface".

Done.

p3 l29 Add after or replace "Numerical" by "thermo-mechanical".

Done.

p4 l12-13 add "M" after "melt rate" add "R" after "Refreezing" and adjust text below.

Done.

p5 l4 It is confusing that the analysis is done with 11 yr moving windows and the lines in the figures are plotted with 30 yr running mean. This makes it difficult to visually inspect the threshold criteria and the location of the dots seems off. Consider revising.

Done. We make the analysis now in a 30-yr moving window and use the 30-yr moving window consistently in the manuscript (Except for the new Fig 5b, where we used for illustration a moving window of 15 years, otherwise we get a constant line for the repeated 30-yr time period). This changed the numbers slightly (HadGEM2-ES from 2021 to 2023 and IPSL-CM5A from 2041 to 2043; MIRCO5 remains at 2009). We have updated the numbers in the text and figures accordingly.

p5 l14 Reformulate "striking". A large scale average will always show less variability compared to a local region in a dynamic system.

Done. We have deleted this sentence.

p5 l25 Conservative interpolation may not be optimal for temperature, a quantity that physically cannot be conserved. I suspect that the imprint of the original GCM grid in the final product we see in Figure 11 and 12 may be related to that. For a vertically downscaled variable, I would not expect such a strong imprint.

Indeed, we have rerun SEMIC with updated input data using bilinear interpolation. This smoothed out the imprint (at least for HadGEM2 and MIROC5; IPSL still shows the imprint). By the way, we found an error for the fields in the Fig. 12 (lower panels). We computed the difference between 2300 and 2100.

p5 l26 Insert "on which SEMIC is run" after "0.05 grid", if that is correct.

Done. This is correct.

p5 l29 Remove line break, still discussing downscaling.

Done.

p6 l7 Add "when MAR is used as forcing" after "best possible SMB and T_s fields".

Done.

p6 l13 Add a figure that shows the absolute SEMIC output, e.g. the 1960-1990 average given in rhs of equation 5.

See answer to MC1.

p6 l20 The integral of deltaSMB in equation 5 from 1960 to 1990 should be zero and the integral of SMB_clim over the same period should be the same for all GCMs. It doesn't look like that in Fig 3, but maybe that is because of the running mean? To check!

We have checked that. The integral from 1960 to 1990 for deltaSMB is zero and SMB_clim is for all 3 GCMs 12001Gt.

p7 l17 Move "integrated" after SMB to avoid confusion between spatial and temporal integration.

Done.

P7 l2 How far are you from the ideal case? Please show that as a figure plotting the difference between the two reference SMBs.

We think, this is not necessary. In a new figure (see answer to MC1) we show the RACMO reference field and the SEMIC-HadGEM2-ES reference field.

p7 l26-29 This text is not part of the validation. Suggest to move to the results section.

As we have rewritten this section and partly restructured this paragraph, this sentence still appear here.

p7 l30 This is not a meaningful validation. See general comments.

See answer to MC1.

p8 l10 This is also not a meaningful validation. See general comments.

See answer to MC1.

p9 l1 The causality of this sentence is not clear to me. Why could an arbitrary time period not be used if absolute SMB would be applied? I believe there may be a fundamental problem arising from the use of the anomaly method. See general comments.

You are right, absolute fields could also be applied. See also answer to MC2.

p9 l3 What is the motivation for using the time period (2250-2280), or is that an arbitrary choice? Please clarify in the text.

See answer to MC2.

p9 27 How do you apply observed velocities to land-terminating glaciers? Only at the ice front, as a boundary condition? Please clarify.

We add “at the ice front”.

p9 l33 This compensation only applies at marine margins, I suppose. Clarify.

No, the compensation applies at marine and land terminating margins. But at land terminating margins melting is compensated. We rewrite to “:... calving and melting exactly compensates …”.

p10 l1 Maybe "have retreated".

Done.

p10 l20 Mention which version of BedMachine.

Done. We use here version 2.

p10 l23 Clarify what noise is expected to be avoided.

Done. We rewrite to “… to avoid spurious noise that arise from errors and biases in the datasets”.

p10 l25 I think it is safe to replace "125 kyr before 1990" by 125 kyr BP, with “(before present)” in first occurrence, to avoid the confusion between 1990 and 1960 in the following.

Done.

p10 l30 Consider discussing the temperature spinup with constant climate after relaxation at p10 l23 and adding it to Table 3.

We think this is not necessary, as it is not relevant for the paper. The spinup with constant climate is just used as a best guess for the initial value for the paleo spinup. See also comment to p11 l20.

p11 9-12 This could be mentioned before describing the method. In any case, reformulate. I don't think you really assume these statements to be true: Replace 'assumptions' by "simplifications". "The currently observed present-day elevation is taken constant for the entire glacial cycle". "the basal friction coefficients obtained from the inversion is taken constant for the past glacial cycle, and (3) the temperature changes from the GRIP record are applied to the whole ice sheet without spatial variations."

Done. The paragraph is moved to the beginning of the initialization approach description and slightly rewritten.

p11 l20 I agree that it may be a negligible effect. But where is the table with comparison of basal temperature against ice core results? The suggestion was not to remove the table, but to check the results that were presented in it.

We have decided to drop the table from the manuscript as it is not relevant for this paper. We are currently working on a manuscript that will present the hybrid spin-up approach in detail.

p12 l27 The drift is ~15% of the magnitude of the lowest projection. That's not negligible. Replace "negligible" by "small".

Done. However, the 15% is calculated to scenario that has almost no change in SMB. Compared to all other scenarios the drift is negligible.

p13 l7-9 Figure 8a and 8b are confused. Exchange.

Done.

p13 l9 Explain blue dots in Figure 8a.

Done. Blue dots represent floating points.

P13 l9 The number in the table rounds to 400 m/a not 390 m/a.

Done.

p13 l11 Was the model run forward in time here or in the comparison, clarify.

Done. We have the sentence rewritten to: The analysis here was done on the original native grid with the high resolution in fast flow regions and on the model was already run forward in time. Compared to this values, the AWI-ISSM results on the regular 5km grid given in Goelzer et al (2017) have a lower RMS value of <20ma^-1.

p13 l13 What is the "assumed critical time"? Clarify.
The “critical time” was introduced in the chapter 2.3 (p8 l7) as “The year 1997 was identified as the critical time of Greenland's peripheral glaciers and ice caps mass balance decrease.” The “critical time” was then again used in chapter 2.6 (p10 l31). So, we don’t change anything here.

p13 l17 Replace "negligible" by "small" and give a number.

Done. The numbers are added “... (-1.4 and -0.7mm for 2100 and 2300, respectively).”.

p13 l20 Replace "variability" by "range". This is an ensemble range.

Done.

p13 l21 Name which figure (Fig 9) after "mass change".

Done.

p13 l22-23 Better discuss only SLE change, otherwise it gets confusing with the different sign of mass and SLE changes.

Done.

p13 l29 The comparison with Fig 1 is hampered by the different reference periods used for temperature and SMB. Consider producing a temperature time series re-referenced to the 1960-1990 reference period.

See answer to MC3.

p14 l3-8 You could mention already here why the numbers are expected to be lower (missing ocean forcing, missing Greenland blocking in GCMs, ...). It seems more appropriate to compare against SMB-only results for this period instead.

Done. In the updated manuscript we show additionally the sea level contribution of 0.4 mm/a from a SMB result (RACMO2.3) and have adjusted the text accordingly: ”Since a future ocean forcing and calving front retreat is not considered here, the response of the ice sheet is likely underestimated here.

Comparing the sea level contributions of each GCM to the sea level contribution of 0.4 mm/a calculated from RACMO2.3 for the same period (dashed black line in Fig. 11) reveals a better agreement. HadGEM2-ES reaches this value 8 years later for RCP2.6 with overshoot and 9 years later for the RCP2.6 scenario without overshoot; IPSL-CM5A 10 years later for RCP2.6 with overshoot."

p14 l9 Shouldn't some of this section 3.3 appear before the projections in chapter 3.2, since it shows the forcing that leads to the ice sheet results?

Done. We have moved this section as suggested.

p14 l16 Replace "cooling" by "less warming", or are you comparing 2300 to 2100? Not always clear what we compare against.

Done. We compare here 2300 with 2100. We have rewritten this sentence.

p14 l20-22 Clarify this contradiction: "amplification is not well represented in MIROC5" <?> "with respect to the Arctic amplification phenomena the most plausible distribution of surface warming is produced by HadGEM2-ES and MIROC5".

Done. The paragraph is rewritten: "Although we do not have a measure to judge future climate warming trends, but with respect to the Arctic amplification phenomena the most plausible distribution and magnitude of surface warming is produced by HadGEM2. By contrast, MIROC5 produces less pronounced warming over Greenland that is similar to the global mean warming but exhibits a plausible pattern of warming. IPSL is spatially and temporally experiencing the largest warming; however, the distribution is not in agreement with the Arctic amplification."

p14 l21- p15 l5 The discussion of realism of future warming patterns remains very speculative and arbitrary.

Yes, we agree. But the discussions about the warming trends highlight the different warming trends and spatial patterns among the used GCMs.

p15 l2-5 The Watterson analysis is probably global, which may not be that meaningful for this Greenland application. This should be mentioned. MIROC5 often scores best when used with MAR compared to other GCMs. This could be mentioned, too.

Done. We mentioned that the Watterson analysis was performed on a global scale.

p15 l21 Remove "increased" before thickening, or was it thickening already?

We delete "increased".

p15 l23 Not sure comparison with observations really holds here. You mean marginal thinning and central thickening as large-scale features? Yes, but the thinning must reach much further inland here. Consider revising.

Done. We rewrite the sentence to: "Generally the large-scale pattern of marginal thinning and central thickening correlates with observations [...]"

p15 l25 Is there evidence from other studies that the 79 glacier is vulnerable? SMB changes in HadCM and MIROC seem very small here and the pattern of retreat looks almost identical. What happens in the unforced control run in this region? Are these changes in the figure also calculated relative to the control run (i.e. double differences)? They should! In any case it may be interesting to inspect and show the control run in a figure.

Done. We have deleted this sentence. The height changes in the Figures are not accounting the control run. We have updated them accordingly but they remain qualitatively the same.

p15 l33-34 Here the discussion of 2100 and 2300 changes is mixed with recent changes.

Done. We have deleted this sentence.

p16 Maybe "ice discharge anomaly"?

Done. As no line number is given we checked all occurrences on page 16 and changed where appropriate.

p17 What is "It"? Clarify.

For the IPSL-CM5A-LR experiment mentioned in the sentence before. We have rewritten this sentence.

Figure 1 The offset between GCMS in temperature in (b) does not correspond with the curves in Fig 3 because of the different reference periods. This makes comparison later in the manuscript difficult and may also have an impact on the timing of the overshoot.

See answer to MC3.

Figure 3 "according to Fig 4.". Replace "thick line" by "solid lines"

Done.

Figure 4 Remove or replace by a more meaningful comparison.
See answer to MC1.

Figure 5 Remove or replace by a more meaningful comparison.

See answer to MC1.

Figure 6 Are values trimmed at +-25? If yes, say so in the caption and give the min/max values.

Done. The values are trimmed.

Figure 8 Explain what the blue dots stand for in a.
Done.
Does an r^2 =1.00 mean perfect correlation? How is that possible?
The value was rounded from 0.99.. to 1.00.

Figure 9 Replace "Straight" by "Solid"

Done.

Figure 10 May want to add an estimate for the SMB-only contribution.

Done. We add a dashed line (0.4mm/a) calculated from RACMO.

References:

Fettweis, X. (2007). Reconstruction of the 1979-2006 Greenland ice sheet surface mass balance using the regional climate model MAR. The Cryosphere, 1(1), 21–40. http://doi.org/10.5194/tc-1-21-2007

Hanna, E., Huybrechts, P., Cappelen, J., Steffen, K., Bales, R. C., Burgess, E., et al. (2011). Greenland Ice Sheet surface mass balance 1870 to 2010 based on Twentieth Century Reanalysis, and links with global climate forcing. Journal of Geophysical Research, 116(D24), n/a–n/a. http://doi.org/10.1029/2011JD016387

Noël, B., Van De Berg, W. J., Machguth, H., Lhermitte, S., Howat, I., Fettweis, X., & Van Den Broeke, M. R. (2016). A daily, 1 km resolution data set of downscaled Greenland ice sheet surface mass balance (1958–2015). The Cryosphere, 10(5), 2361–2377. http://doi.org/10.5194/tc-10-2361-2016

Vernon, C. L., Bamber, J. L., Box, J. E., Van Den Broeke, M. R., Fettweis, X., Hanna, E., & Huybrechts, P. (2013). Surface mass balance model intercomparison for the Greenland ice sheet. The Cryosphere, 7(2), 599–614. http://doi.org/10.5194/tc-7-599-2013

The effect of overshooting 1.5°C global warming on the mass loss of the Greenland Ice Sheet

Martin Rückamp[1], Ulrike Falk[2], Katja Frieler[3], Stefan Lange[3], and Angelika Humbert[1,4]

[1]Alfred Wegener Institute, Helmholtz Centre for Polar and Marine Research, Bremerhaven, Germany
[2]formerly Alfred Wegener Institute, Helmholtz Centre for Polar and Marine Research, Bremerhaven, Germany
[3]Potsdam Institute for Climate Impact Research, Potsdam, Germany
[4]University of Bremen, Bremen, Germany

Correspondence to: martin.rueckamp@awi.de

Abstract. Sea level rise associated with changing climate is expected to pose a major challenge for societies. Based on the efforts of COP21 to limit global warming to 2.0°C or even 1.5°C by the end of 21$^{\text{th}}$ century (Paris Agreement), we simulate the future contribution of the Greenland ice sheet (GrIS) to sea level change under the low emission representative concentration pathway (RCP) 2.6 scenario. The ice sheet model ISSM with higher order approximation is used and initialized with a hybrid approach between spin-up and data assimilation. For three general circulation models (HadGEM2-ES, IPSL-CM5A-LR, MIROC5) the projections are conducted up to 2300 with forcing fields for surface mass balance (SMB) and ice surface temperature (T_s) computed by the ~~SEMIC model~~ surface energy balance model SEMIC (Krapp et al., 2017). The projected sea level rise ranges between 21–38 mm by 2100 and 36–85 mm by 2300. According to the three GCMs used, warming of 1.5°C ~~has been~~ will be exceeded early in the 21$^{\text{th}}$ century. The RCP2.6 peak and decline scenario is therefore in a another set of experiments manually adjusted to suppress the 1.5°C-overshooting effect. These scenarios show a sea level contribution that is on average about 38% and 31% less by 2100 and 2300, respectively. The rate of mass loss in the 23$^{\text{rd}}$ century is for some ~~scenarios~~ experiments not excluding a stable ice sheet in the future. This is ~~most likely due to an integrated~~ due to a spatial-integrated SMB that never ~~fall~~ falls below zero, or even a recovery of SMB towards values of slightly below present day. Although the mean SMB is reduced in the warmer climate, a future steady-state ice sheet with lower surface elevation and hence volume might be possible. Our results indicate, that uncertainties in the projections stem from the underlying ~~climate model~~ GCM climate data to calculate the surface mass balance. However, the RCP2.6 scenario will lead to significant changes of the GrIS including elevation changes of up to 100 m. The sea level contribution estimated in this study may serve as a lower bound for the RCP2.6 scenario, as the current observed ~~observed~~ sea level rise is ~~in none~~ not reached in any of the experiments~~reached~~; this is attributed to processes (e.g. ocean forcing) not yet represented by the model but proven to play a major role in GrIS mass loss.

1 Introduction

Within the past decade the Greenland ice sheet (GrIS) has contributed by about 20% to sea level rise (Rietbroek et al., 2016) and ~~global sea level rise has just recently shown to accelerate (Nerem et al., 2018)~~its future contribution poses a major societal challenge. The mass loss of ~~GrIS comprises two main contributions: acceleration of outlet glaciers and~~ the ice sheets to global sea level rise is caused by changes in the surface mass balance ~~. In~~ and acceleration of outlet glaciers (Nerem et al., 2018). For the past decades~~these changes in surface mass balance contributed~~ , the relative contributions are estimated to about 60% ~~, whereas~~ and 40%~~is attributed to increasing discharge~~ , respectively (van den Broeke et al., 2016). The question arises which impact the GrIS will have on ~~global and regional~~ sea level change in the next decades and centuries.

Negotiated during COP21, the Paris Agreement's aim is to keep a global temperature rise in this century well below 2°C above pre-industrial levels and to pursue efforts to limit the temperature increase even further to 1.5 degrees Celsius (UNFCCC, 2015). However, the statement holding global temperature below 2°C implies keeping global warming below the 2°C limit over the full course of the century and afterwards while efforts to limit the temperature increase to 1.5°C is often interpreted as allowing for a potential overshoot before returning to below 1.5°C (Rogelj et al., 2015). Here we selected the Representative Concentration Pathways (RCP, Moss et al., 2010) 2.6, being the lowest emission scenario considered within CMIP5 and in line with a 1.5°C or 2°C limit of global warming. Depending on the global circulation models (GCM) considered the global temperature change over time varies considerably although the political target is met at 2100. Whereas some models in RCP2.6 are not passing the limit of 1.5°C or 2.0°C global warming before 2100, other ~~scenarios~~ models cross this limit and exhibit subsequent cooling (Frieler et al., 2017).

While global temperature rise may be limited to 1.5°C or 2°C by 2100, warming over Greenland is enhanced due to the Arctic amplification (Pithan and Mauritsen, 2014) and ~~may exceed 4°C by that time and~~ has exceeded 1.5°C (relative to 1951–1980) already in the past decade (GISTEMP Team, 2018) ~~. Given that this~~ and may exceed 4°C by that time. This is about more than 2°C ~~above the~~ warming by 2000 ~~this could have an~~ and could therefore have a considerable impact on ice sheet mass loss over Greenland. This implies an enlargement of the ablation zone and goes along with a decline in SMB. However, it is currently unclear, how fast GrIS could react to cooling and recovery of SMB, as ice sheets are also reacting dynamically to atmospheric forcing.

Recent large-scale ice sheet modelling attempts for projecting the contribution of the GrIS under RCP2.6 warming scenarios are very scarce. Fürst et al. (2015) conducted ~~a very~~ an extensive study to simulate future ice volume changes driven by both atmospheric and oceanic temperature changes for all four representative concentration pathway scenarios. For the RCP2.6 scenario they estimate an abated sea level contribution of 42.3±18.0 mm by 2100 and 88.2±44.8 mm by 2300. The value by 2100 is in line with estimates given by the Fifth Assessment Report of the Intergovernmental Panel on Climate Change (IPCC AR5, IPCC (2013)). The AR5 range for RCP2.6 is between 10-100 mm by 2100 (the value is dependent whether ice-dynamical feedbacks are considered or not).

The GrIS response to projections of future climate change are usually studied with a numerical ice sheet model (ISM) forced with climate data. ISM response is subject to the dynamical part and the surface mass balance (SMB). In the past,

ISMs often used the rather simple and empirical based positive degree day (PDD) scheme, in which the PDD index is used to compute melt, run-off and ice surface temperature from atmospheric temperature and precipitation (Huybrechts et al., 1991). One disadvantage of the PDD method is, that the involved PDD parameters are tuned to correctly represent present-day melting rates but may fail to represent past or future climates (Bougamont et al., 2007; Bauer and Ganopolski, 2017). On one far end of model complexity, a regional climate model (RCM) resolves most processes at the ice-atmosphere interface and in the upper firn layers, such as RACMO (Noël et al., 2018) or MAR (Fettweis et al., 2017) with higher spatial and temporal resolution than GCMs. RCMs have been shown to be quite successful in reproducing the current SMB of the GrIS. However, as they are computationally expensive, an intermediate way would be ~~most suitable~~more efficient, balancing computational costs and ~~parameterisation~~ parameterization of processes, such as the energy balance model of intermediate complexity ~~, like~~ SEMIC (Krapp et al., 2017).

Here we target in particular RCP2.6 peak and decline scenarios in order to study the GrIS response on overshooting by means with an numerical ISM. The projections are driven with climate data output from the CMIP5 RCP2.6 scenario provided by the ISIMIP2b project for different GCMs (Frieler et al., 2017). To obtain ice surface temperature and surface mass balance from the atmospheric fields, the surface energy balance model SEMIC (Krapp et al., 2017) is applied. The SEMIC model (Sect. 2.1) is driven ~~offline~~ off-line to the ISM and therefore the climate forcing is one-way coupled and applied as anomalies to the ISM. The advantage of this one-way coupling is the lower computational costs, allowing for reasonably high spatial and temporal resolution of the ISM. In order to study the effect of overshooting, we design a RCP2.6-like scenario without an overshoot by manually stabilizing the forcing at 1.5°C.

For modelling the flow dynamics and future evolution of the GrIS under RCP2.6 scenarios, the thermo-mechanical coupled Ice Sheet System Model (ISSM, Larour et al., 2012) with a Blatter-Pattyn type higher order momentum balance (BP; Blatter, 1995; Pattyn, 2003) is applied (Sect. 2.5). A crucial prerequisite for projections is a reasonable initial state of the ice sheet in terms of ice ~~volume~~thickness, ice extent and ice ~~surface~~ velocities. Beside starting projections with the most realistic setting, the prevention of a model shock after switching from the initialization procedure to projections, is very important. Both has been a major issue in the past, which gave rise to an international benchmark experiment initMIP Greenland (Goelzer et al., 2018) for finding optimal strategies to derive initial states for the ice velocity and temperature fields. ~~Using~~ Here, we apply a hybrid approach ~~of~~ between a thermal paleo-spin up and data assimilation~~has been shown to be a good way and is applied here~~.

Before driving the projections, the SMB forcing is validated thoroughly against RACMO. Then we explore the response of the GrIS and its contribution to sea-level rise under RCP2.6 scenario ~~with overshoot and an~~ and a modified RCP2.6 scenario without overshoot.

2 Model description

2.1 Energy Balance Model

~~Numerical~~ Thermo-mechanical ISMs need the annual mean surface temperatures and annual mean surface mass balance of ice as boundary conditions at the surface. To derive these ice sheet specific quantities, we use the surface energy balance model

of intermediate complexity (SEMIC, Krapp et al., 2017). Although we only apply SEMIC and do neither adjust parameters of SEMIC, SEMIC is described very briefly. SEMIC computes the mass and energy balance of snow and/or ice surface. In order to tune parameters for a number of processes, ~~(Krapp et al., 2017) performed an optimisation~~ Krapp et al. (2017) performed an optimization for the GrIS based on reconstruction and regional climate model data. These parameters have been used in our study, too. The energy balance equation reads as

$$c_{\text{eff}} \frac{\mathrm{d}T_\mathrm{s}}{dt} = (1-\alpha) \cdot \mathrm{SW}^{\downarrow} - \mathrm{LW}^{\uparrow} + \mathrm{LW}^{\downarrow} - H_\mathrm{S} - H_\mathrm{L} - Q_{\mathrm{M/R}}\,, \tag{1}$$

where α is the surface albedo that is parameterized with the snow height (Oerlemans and Knap, 1998). The downwelling shortwave $\mathrm{SW}^{\downarrow}$ and downwelling longwave radiation $\mathrm{LW}^{\downarrow}$ at the surface are provided as atmospheric forcing (sect. 2.2). The upwelling longwave radiation $\mathrm{LW}^{\uparrow}$ is described by the Stefan-Boltzmann law. The latent H_L and sensible H_S heat fluxes are estimated by the respective bulk approach (e.g. Gill, 1982). The residual heat flux $Q_{\mathrm{M/R}}$ is calculated from the difference of melting M and refreezing R and keeps track of any heat flux surplus or deficit in order to keep the ice surface temperature T_s below or equal to 0°C over snow and ice.

The surface mass balance SMB in SEMIC is considered as follows

$$\mathrm{SMB} = P_\mathrm{s} - SU - M - R\,, \tag{2}$$

where P_s is the rate of snowfall and SU the sublimation rate, which is directly related to the latent heat flux. The melt rate M is dependent on the snow height, if all snow is melted down the excess energy is used to melt the underlying ice. Refreezing R is calculated differently for available melt water or rainfall. Moreover, the porous snowpack could retain a limited amount of meltwater while over ice surfaces refreezing is neglected and all melted ice is treated as run-off. In SEMIC, the total melt rate ~~M~~ and refreezing rate ~~R~~ are calculated from available energy during the course of one day. As the set of equations are solved using an explicit time-step scheme with a time step of one day, a parametrization for the diurnal cycle (a cosine function) account for thawing and freezing over a day. This reduced complexity, one-layer snowpack model saves computation time and allows for integrations on multi-millennial timescales compared to more sophisticated multilayer snowpack models. Further details are given by Krapp et al. (2017).

2.2 Atmospheric forcing

Here we targeted in particular peak and decline scenarios, temporarily exceeding a given temperature limit of global warming to 2.0°C or even 1.5°C by the end of 2100. From the official extended RCP2.6 scenarios (Meinshausen et al., 2011), we have selected GCMs which ~~covering~~ cover the CMIP5 historical scenario, the RCP2.6 scenario until 2299 and reveal an overshoot in annual global mean near-surface temperature change relative to pre-industrial levels (1661–1860). Three different GCMs were used in our study: IPSL-CM5A-LR (L'Institut Pierre-Simon Laplace Coupled Model, version 5 (low resolution)), MIROC5 (Model for Interdisciplinary Research on Climate, version 5) and HadGEM2-ES (Hadley Centre Global Environmental Model 2, Earth System). Instead of the full acronyms we use IPSL, HadGEM2 and MIROC5 in the following text. The

GCM output was provided and prepared by the ISIMIP2b project following a strict simulation protocol (Frieler et al., 2017). Figure 1a displays the temporal evolution of the annual global mean near-surface air temperature T_a for those GCMs for the historical simulation up to 2005 continued with the RCP2.6 simulation up to 2299. Global-mean-temperature projections from ~~IPSL-CM5A-LR and HadGEM2-ES~~ IPSL and HadGEM2 under RCP2.6 exceed 1.5°C relative to pre-industrial levels in the second half of the 21st century. While global-mean-temperature change returns to 1.5°C or even slightly lower by 2299 in ~~HadGEM2-ES~~HadGEM2, it only reaches about 2°C in ~~IPSL-CM5A-LR~~ IPSL by 2299. For MIROC5, it stabilizes at about 1.5°C during the second half of the 21st century. In order to determine the onset of overshoot we scan the historical and RCP2.6 scenarios of the individual GCMs identifying the time, when the global warming reaches 1.5°C in a ~~11-year~~ 30-year moving window above pre-industrial levels. The characteristic dates of overshooting 1.5°C for ~~HadGEM2-ES is by 2021~~HadGEM2 is by 2023; MIROC5 reaches this level by ~~2041, while IPSL-CM5A-LR~~ 2043, while IPSL reaches this point by 2009 (~~coloured~~ colored dots in Fig. 1).

The phenomenon, that tends to produce a larger change in temperature near the poles was termed polar amplification. Particularly, it enhances the increase in global mean air temperature over arctic areas (referred here as arctic amplification). Generally, the the CMIP5 models show an annual average warming factor over the Arctic between 2.2 and 2.4 times the global average warming (IPCC, 2013, Tab. 12.2). As mechanisms creating the arctic amplification may be represented to different extents in the GCMs, the level of future amplification is different across the GrIS. The three GCMs used in this study represent this trend to differing extents over GrIS[1,2] (Fig. 1 and 2). For ~~HadGEM2-ES and IPSL-CM5A-LR~~ HadGEM2 and IPSL the arctic compared to the global warming is amplified relatively similar (warming approx. 4°C relative to 1661–1860). In contrast, MIROC5 reveals a considerably lower arctic amplification (warming approx. 3°C relative to 1661–1860). ~~A striking feature among all models is the higher variability over GrIS compared to the global mean values.~~ In terms of global and arctic future annual mean near-surface temperatures MIROC5 is the lowest and ~~IPSL-CM5A-LR~~ IPSL the highest forcing.

The ISIMIP2b atmospheric forcing data are CMIP5 climate model output data that have been spatially interpolated to a regular 0.5°×0.5° latitude-longitude grid and bias-corrected using the observational dataset EWEMBI (Frieler et al., 2017; Lange, 2017). To drive the SEMIC model to obtain the ice surface temperature T_s of the ice sheet and the surface mass balance SMB we need to provide the atmospheric forcing (consisting of incoming shortwave radiation $SW^{\downarrow}$, longwave radiation $LW^{\downarrow}$, near-surface air temperature T_a, surface wind speed u_s, near-surface specific humidity q_a, surface air pressure p_s, snowfall rate P_s, and rainfall rate P_r). These fields are available from the three GCMs model output data. SEMIC is driven by the daily input of the GCMs while the output is a cumulative surface mass balance and a mean surface temperature over each year.

Given the differences in resolution between the GCMs and ISSM, a vertical downscaling procedure is applied to the atmospheric forcing fields. First the atmospheric fields are ~~conservatively~~ bilinear interpolated from the GCM grid onto a regular high resolution 0.05° grid on which SEMIC is run. The output fields of SEMIC are subsequently conservatively interpolated on the unstructured ISSM grid. This two-step procedure is not necessary but currently it is ~~technical~~ technically the easiest way. For future applications we will avoid the intermediate interpolation and run SEMIC directly on the target unstructured ISSM grid.

Table 1. Lapse rates and height-desertification relationship for initial corrections of GCM output fields near-surface air temperature T_a, precipitation of snow P_s, precipitation of rain P_r, and downwelling longwave radiation $LW^{\downarrow}$ used as input for SEMIC. Here, h^{ref} = 2000 m is the reference height and $\gamma_p = -0.6931\,\mathrm{km}^{-1}$ is the desertification coefficient.

variable	lapse ~~rate~~ rates γ and desertification relationship	reference
T_a	0.74 K/100 m	Erokhina et al.
$LW^{\downarrow}$	2.9 W m^{-2}	Vizcaíno et al.
P_s, P_r	~~$\exp(\gamma_p[\max(h_s^{\mathrm{ISSM-pd}}, h^{\mathrm{ref}}) - h^{\mathrm{ref}}]) \quad \forall \quad h_s^{\mathrm{GCM}} \leq h^{\mathrm{ref}}$~~ $\exp(\gamma_p[\max(h_s^{\mathrm{SEMIC}}, h^{\mathrm{ref}}) - h^{\mathrm{ref}}]) \quad \forall \quad h_s^{\mathrm{GCM}} \leq h^{\mathrm{ref}}$	Vizcaíno et al.
P_s, P_r	~~$\exp(\gamma_p[\max(h_s^{\mathrm{ISSM-pd}}, h^{\mathrm{ref}}) - h_s^{\mathrm{GCM}}]) \quad \forall \quad h_s^{\mathrm{GCM}} > h^{\mathrm{ref}}$~~ $\exp(\gamma_p[\max(h_s^{\mathrm{SEMIC}}, h^{\mathrm{ref}}) - h_s^{\mathrm{GCM}}]) \quad \forall \quad h_s^{\mathrm{GCM}} > h^{\mathrm{ref}}$	Vizcaíno et al.

To account for the difference in ice sheet surface topography between GCMs and ISSM corrections for several quantities $(\cdot)$ denoted by $(\cdot)^{\mathrm{cor}}$ are initially performed. We follow the corrections proposed by Vizcaíno et al. (2010)

$$(\cdot)^{\mathrm{cor}} = (h_s^{\mathrm{SEMIC}} - h_s^{\mathrm{GCM}})\gamma_{(\cdot)}, \tag{3}$$

with the lapse rates $\gamma_{(\cdot)}$ shown in ~~Table~~ Tab. 1 and h_s^{SEMIC} is equal the ISSM ice surface elevation at the initial state. Subsequently, SEMIC computes the ice-surface temperature T_{s} and the surface mass balance ~~SMB~~ SMB based on these corrected input values.

SEMIC is applied as developed by Krapp et al. (2017). These authors perform a particle-swarm optimization to calibrate model parameters for the GrIS and validate them against the RCM MAR. We adopt their derived parameters here. The parameter tuning aimed to find a parameter set which gives a best fit between SMB and ice temperature T_{s} of SEMIC with only a limited number of processes and simpler ~~parameterisations~~ parameterizations compared to a more complex RCM. A RCM is typically validated against reanalysis data and observations, therefore, we assume the tuned parameters are most reliable to represent the processes and ~~parametrizations~~ parameterizations within SEMIC. In terms of process description the optimized SEMIC configuration leads to the best possible SMB and T_{s} fields ~~. However, although the coarse GCM-based forcing has underwent a downscaling of particular fields and is processed in SEMIC with a higher resolution the atmospheric fields over the ice sheet still lacks details and quality compared to a RCM . Given the experiences we made with GCMs used in this study~~ when MAR is used as forcing. If SEMIC is tuned with another RCM (e.g. RACMO or HIRHAM), the parameter will be different. Here, a separate tuning for each GCM would be required due to the differences (e.g. the timing of maximum warming, the length of an overshoot) ~~would require a separate tuning for each GCM~~among the GCMs used in this study. This basically means to compensate, for e.g. too low near surface temperatures, with SEMIC parameters, which would offset the whole comparison of GCM forcing. Furthermore, this additional tuning steps would make the benefit of having a semi-complexity model with low costs meaningless.

~~Because the details of the GrIS surface climate are not well captured on the GCM coarse grid, the absolute SEMIC~~ However, Figure 3 compares averaged SMB fields for the time period 1960–1990 from RACMO2.3 and exemplary the SMB derived by forcing SEMIC with HadGEM2. The pattern of the SMB derived by forcing SEMIC with IPSL or MIROC5 is the same

as using HadGEM2. The comparison in Fig. 3 shows that the large-scale pattern of the SMB fields agree fairly well while the small-scale pattern and magnitudes of the GCM-based SMB is not in agreement with the RACMO2.3 SMB. Although the coarse GCM-based forcing has underwent a downscaling of particular fields and is processed in SEMIC with a higher resolution the atmospheric fields over the ice sheet still lacks details and quality compared to a RCM. This is due to the fact, that the forcing from a GCM implies different characteristics, like smoother gradients and less resolved geometry compared to the RCM. The direct output of the SMB from SEMIC to the RACMO2.3 field has a misfit of about 2 m a^{-1} and a correlation coefficient of R^2=0.5. Additionally, the spatial-integrated SMB for the averaged time period differs up to 200 Gt a^{-1}; for HadGEM2, IPSL and MIROC5 the values are 536, 496, and 614 Gt a^{-1}, respectively. In contrast, the corresponding value for RACMO2.3 is 403 Gt a^{-1}. Therefore, we conclude that the absolute fields from SEMIC are not ideal for our purpose.

Instead of using the absolute SEMIC output fields (SMB and T_s) ~~are not directly used~~ directly to force the numerical ice flow model ISSM, we rely on an anomaly method. The climatic boundary conditions applied here consist of a reference field onto which climate change anomalies from SEMIC are superimposed. The initialization of the ice flow model based on data assimilation (Sect. 2.6 below) makes it possible to use forcing data from high resolution RCMs that were run on the same ice sheet mask and ice surface topography. As the reference SMB field we choose the downscaled RACMO2.3 product (Noël et al., 2018) whereby a model output was averaged for the time period 1960–1990, denoted $\overline{\mathrm{SMB}}(1960-1990)_{\mathrm{RACMO}}$. The reference period 1960–1990 is chosen as the ice sheet is assumed close to steady state in this period (e.g. Ettema et al., 2009). The climatic SMB that is used as future climate forcing read as

$$\mathrm{SMB}_{\mathrm{clim}}(x,y,t) = \overline{\mathrm{SMB}}^{(1960-1990)}_{\mathrm{RACMO}}(x,y) + \Delta\mathrm{SMB}(x,y,t), \tag{4}$$

with the anomaly defined as

$$\Delta\mathrm{SMB}(x,y,t) = \mathrm{SMB}_{\mathrm{SEMIC}}(x,y,t) - \overline{\mathrm{SMB}}^{(1960-1990)}_{\mathrm{SEMIC}}(x,y), \tag{5}$$

where t={1960, 1961, ... , 2299}. Note that the historical scenario is run from 1960–2005 and followed by the RCP2.6 scenario from 2006–2299. In an ideal case, both reference terms $\overline{\mathrm{SMB}}(1960-1990)_{\mathrm{RACMO}}$ and $\overline{\mathrm{SMB}}(1960-1990)_{\mathrm{SEMIC}}$ will cancel out and the absolute climatic forcing $\mathrm{SMB}_{\mathrm{SEMIC}}(x,y,t)$ would remain. This is certainly not the case and the equation must be interpreted as having the ~~RACMO~~ RACMO2.3 reference field (with a good spatial distribution) as a background field with the trends from SEMIC superimposed.

The same equations hold for the temperature imposed on the ice-surface. This ensures that the unforced control experiment produces identical ~~behaviour~~ behavior for each GCM. Results for future projections depend only on the atmospheric GCM input, or similarly SEMIC output, and therefore the results can be compared quantitatively. In the following text, the constructed SMB fields according to Eq. 4 are referred as SEMIC-HadGEM2, SEMIC-IPSL and SEMIC-MIROC5 or in general as SEMIC-GCM.

In the presented study, the ice flow model is forced with the ~~offline~~ off-line processed SEMIC output. This one-way coupling strategy is computational cheaper and the technically challenging ~~online~~ on-line coupling is avoided. However, as the ice sheet evolves in response to climate change, local climate feedback processes are not captured. Most importantly the interaction of

the ice surface between air temperature and precipitation, which in turn affects the surface mass balance. The ~~SMB-feedack~~ SMB-feedback process is considered with a dynamic correction to the $\mathrm{SMB_{clim}}$ (see sect. 2.7 below). This correction is applied within ISSM and to the surface mass balance term only.

2.3 ~~Validation of SMB forcing~~Modified RCP2.6 scenario without overshoot

The global climate warming of the selected GCMs exceeds the political target of 1.5°C during the 20$^{\mathrm{th}}$ century although the RCP2.6 is the strongest mitigation scenario focusing on negative emissions (Moss et al., 2010). In order to ~~validate the obtained~~ estimate the overshooting effect on the projected sea level contribution from the GrIS we manually construct a RCP2.6-like scenario without an overshoot assuming an immediate climate stabilization at that time when 1.5°C is reached. As mentioned before, we identify the time when the global warming reaches 1.5°C in a 30-year moving window above pre-industrial levels. The characteristic times of overshooting 1.5°C for HadGEM2 is by 2023; MIROC5 reaches this level by 2043, while IPSL reaches this point by 2009. Before reaching these threshold the unaltered historical and RCP2.6 forcing is applied. The extension of the forcing from these characteristic times is of crucial importance. To avoid an unphysical step change the climate in the repeated time period should stabilize (i.e. no long term trends in temperature change) close to 1.5°C warming. In order to account for decadal variability, i.e. extreme years, we reuse the climatic forcing fields from 2250–2280 until the end of the simulation (light gray shaded areas in Fig. 1 and 4). In this time window, the warming is close to 1.5°C and exhibits a frequent number of extreme years. Other time widows might also be feasible (e.g. the last 30 or 50 years) but will likely not change the forcing substantially. In the following, the modified RCP2.6-like scenario without overshoot is termed as RCP2.6 without overshoot.

2.4 Assessment of SMB forcing

We want to emphasize that we do not intend to validate the energy balance model SEMIC itself, but assess if the obtained SMB fields by forcing SEMIC with the GCMs are plausible. In order to do so the obtained climatic $\mathrm{SMB_{clim}}$ (Eq. 4), the resulting SMB patterns and time series are compared with other available data-sets. Beside the spatial pattern of the surface mass balance, the time series of the ~~integrated~~ SMB over Greenland ~~illustrate~~ illustrates what the ice sheet's total surface gains and losses have been over the year from SMB~~(~~. The constructed SMB forcing for the RCP2.6 scenario with and without overshoot are shown in Fig. 4~~). The grey~~ a and b, respectively. The gray shaded box and black line depicts the range and the mean SMB between 1981–2010 from ~~Polarportal~~ polarportal (polarportal.dk) derived from a combination of observations and a weather model for Greenland (Hirlam-Newsnow). The dashed black line shows the results from the RACMO2.3 product. The ~~integrated~~ spatial-integrated SMB magnitude of each ~~GCM~~ SEMIC-GCM is consistent with the RACMO2.3 and polarportal data. The drop in SMB after 2000 is present in all three ~~GCMs and RACMO. The decline of SMB roughly corresponds with MAR results forced with the GCM NorESM1-M under RCP2.6 scenario (Fettweis et al., 2013, last column in Tab. 2), although it is not strictly comparable because they use a different GCM climate data. They estimated a loss of -124 ± 100 Gt a^{-1} in 2080–2099 relative to 1980–1999.~~ SEMIC-GCMs and RACMO2.3.

For ~~HadGEM2-ES the integrated~~ SEMIC-HadGEM2 the spatial-integrated SMB remains around 200 Gt a^{-1} after 2050. The SMB for ~~IPSL-CM5A-LR~~ SEMIC-IPSL recovers from 2050 onwards and shows an increase from around 200 Gt a^{-1} to around 350 Gt a^{-1} by 2300. ~~MIROC5~~ SEMIC-MIROC5 reveals the lowest SMB change over time and recovers after 2050 from 250 Gt a^{-1} to 300–350 Gt a^{-1} by 2300. The SMB of ~~IPSL-CM5A-LR and MIROC5~~ SEMIC-IPSL and SEMIC-MIROC5 is by 2300 ~~almost of similar magnitude as~~ slightly below the magnitude of present-day.

~~For the available RACMO2.3 time series we have computed the coefficient of determination r^2 and the mean signed difference (MSD) for surface mass balance, accumulation and melt (Fig.5). The interannual SMB variability agrees well and the MSD oscillates around zero and with values up to~~ However, the decline of SMB for the RCP2.6 scenario roughly corresponds with MAR results forced with the GCM NorESM1-M under RCP2.6 scenario (Fettweis et al. (2013) and last column in Tab. 2), although it is not strictly comparable because they use different GCM climate data. They estimated a loss of -124±~~0.5~~100 ~~mGt~~ a^{-1} ~~(Fig.5a). For the time period 1960–2016 the overall surface mass balance difference over the ice sheet between SEMIC and RACMO is almost zero with -0.007 m a^{-1} , 0.016 m a^{-1} and 0.0200 m a^{-1} for HadGEM2-ES, IPSL-CM5A-LR and MIROC5, respectively. These numbers are in the same range as given by Krapp et al. (2017) for the comparison between SEMIC and MAR. Nonetheless, averaging the MSD over the whole time period the surface accumulation agrees better compared to surface melt (surface accumulation: -0.034 m a^{-1}, -0.031 m a^{-1}, -0.023 m a^{-1}; surface melt: 0.048 m a^{-1}, 0.066 m a^{-1}, 0.061 m a^{-1}). The coefficient of determination is larger than 0.8 for all components except with some outliers.~~ in 2080–2099 relative to 1980–1999.

Table 2 shows annual mean integrated SMB over the entire GrIS for various periods. Averaged over most of the periods the annual mean integrated SMB is among the ~~model~~ models rather similar. Most obvious are the differences between the ~~GCMs~~ SEMIC-GCMs for the period 1997–2016. The year 1997 was identified as the critical time of Greenland's peripheral glaciers and ice caps mass balance decrease (Noël et al., 2017). For this period of declining SMB the ~~HadGEM2-ES~~ SEMIC-HadGEM2 agrees well to the RACMO2.3 product while the spatial-integrated SMB for SEMIC-IPSL and SEMIC-MIROC5 are ∼40 and 50 Gt a^{-1} larger, respectively. In general the compared values over all time periods agree fairly well.

~~The validation include an analysis of the spatial pattern of SMB. Here we compare exemplary the spatial pattern of RACMO2.3 for the year 1990 against the SMB derived from HadGEM2-ES for the year 1990 (Fig. 3). The maps show, that accumulation and ablation patterns agree reasonably well. The SMB patterns for other GCMs or time slices are qualitatively similar but deviate in absolute values as the annual variability is not coherent among all models.~~

2.5 ~~Modified RCP2.6 scenario without overshoot~~

~~The global climate warming of the selected GCMs exceeds the political target of 1.5°C during the 20th century although the RCP2.6 is the strongest mitigation scenario focussing on negative emissions (Moss et al., 2010). In order to estimate the overshooting effect on the projected sea level contribution from the GrIS we manually construct a RCP2.6-like scenario without an overshoot assuming an immediate climate stabilisation at that time when 1.5°C is reached. As mentioned before, we identify the time when the global warming reaches 1.5°C in a 11-year moving window above pre-industrial levels.The characteristic times of overshooting 1.5°C for HadGEM2-ES is by 2021; MIROC5 reaches this level by 2041, while IPSL-CM5A-LR by~~

Table 2. Annual mean integrated SMB ($Gt\,yr^{-1}$) covering various periods. Time series of SMB_{clim} for the ~~GCMs~~ SEMIC-GCMs are calculated by Eq. 4 for RCP2.6 scenario~~with overshoot~~. The column '1.5°C reached' gives an ~~11-year~~ 30-year mean at the characteristic time of overshooting 1.5°C. Anomaly in SMB (ΔSMB) is in 2080–2099 with respect to 1980–1999.

Model	1960–1990	1960–1997	1997–2016	1981–2010	1960–2016	1.5°C reached	ΔSMB
RACMO2.3	402.8	403.4	279.1	363.1	364.8	-	-
polarportal	-	-	-	370	-	-	-
MAR [a]	-	-	-	-	-	-	−124±100
~~HadGEM2-ES~~ SEMIC-HadGEM2	400.0	391.2	277.0	358.1	355.2	170.0	−179.2
~~IPSL-CM5A-LR~~ SEMIC- IPSL	408.9	412.5	332.8	403.7	382.2	363.9	−170.4
~~MIROC5~~ SEMIC-MIROC5	395.0	398.5	341.2	341.8	380.0	288.4	−80.9

[a] MAR forced with GCM NorESM1-M under RCP2.6 scenario (Fettweis et al., 2013)

~~2009. Before reaching these threshold the unaltered historical and RCP2.6 forcing is applied. The extension of the forcing from these characteristic times is of crucial importance. Since the forcing is constructed by using the GCM trends instead of absolute values an arbitrary time period can be used. In order to account for decadal variability and assuming a stabilized climate we reuse the climatic forcing fields from 2250–2280 until the end of the simulation (light grey shaded areas in Fig. 1 and 4). At the characteristic times the three GCMs reveal a SMB that differs up to 200~~For the available RACMO2.3 time series we have computed the interannual SMB variability for RACMO2.3 and the SEMIC-GCMs (Fig. 5). The SMB variability is in terms of frequency and amplitude similar to RACMO2.3 but is not coherent among all models because the GCMs have their own internal variability. For the time period 1960–2016 the overall surface mass balance difference over the ice sheet between SEMIC-GCM and RACMO2.3 is almost zero with -0.007 ~~Gtm yr~~a^{-1} ~~(Column '1.5°C reached' in Tab. 2). While HadGEM2-ES has declined to 170~~, 0.016 ~~Gtm yr~~a^{-1} ~~, IPSL-CM5A-LR remains with 363.9~~and 0.0200 ~~Gtm yr~~a^{-1} ~~relatively close to present-day. In the following, the modified RCP2.6-like scenario without overshoot is termed as RCP2.6 without overshoot~~for SEMIC-HadGEM2, SEMIC-IPSL and SEMIC-MIROC5, respectively. These numbers are in the same range as given by Krapp et al. (2017) for the comparison between SEMIC and MAR.

2.5 Ice flow model

Ice flow and thermodynamic evolution of the GrIS are approximated using the finite-element ISSM. The model has been applied successfully to both large ice sheets (Bindschadler et al., 2013; Nowicki et al., 2013; Goelzer et al., 2018) and is also used for studies of individual drainage basins of Greenland, e.g. the North East Greenland Ice Stream (Choi et al.), Jakobshavn Isbræ (Bondzio et al., 2016, 2017) and Store Glacier (Morlighem et al., 2016). Here, we use an incompressible non-Newtonian constitutive relation with viscosity dependent on temperature, microscopic-water content and strain rate, while neglecting the softening effect of damage or impurities. The BP approximation to the Stokes momentum balance equation is employed in order to account for longitudinal and transverse stress gradients.

ISSM is specified with kinematic boundary conditions at the upper and lower boundary of the ice sheet. The upper boundary incorporates the climatic forcing, i.e. the surface mass balance and ice surface temperature, while the base of the ice is specified as both impenetrable with the bedrock and in balance with the rate of melting. The basal melt rate below ice shelves is ~~parameterised~~ parameterized with a Beckmann-Goosse relationship (Beckmann and Goosse, 2003). The melt-factor is roughly adjusted such that melting rates corresponds to literature values (e.g. Wilson et al., 2017). Within this study the basal melt rate is not a focus and hence the basal melt underneath floating tongues or vertical calving fronts of tidewater glaciers are not changed. Once the pressure melting point at the grounded ice is reached melting is calculated from basal frictional heating and the heat flux difference at the ice/bed interface At the ice base sliding is allowed everywhere and the basal drag, $\boldsymbol{\tau}_b$, is written using Coulomb friction:

$$\boldsymbol{\tau}_b = -k^2 N \boldsymbol{v}_b, \tag{6}$$

where $\boldsymbol{v}_b$ is the basal velocity vector tangential to the glacier base and k^2 a constant. The effective pressure is defined as $N = \varrho_i\, g\, H + \varrho_w\, g\, h_b$, where H is the ice thickness, h_b the glacier base and $\varrho_i = 910\,\mathrm{kg\,m^{-3}}$, $\varrho_w = 1028\,\mathrm{kg\,m^{-3}}$ the densities for ice and sea water, respectively. We apply water pressure at the calving front of marine terminating glaciers and observed surface velocities (Rignot and Mouginot, 2012) at the ice front of land terminating glaciers. A traction-free boundary condition is imposed at the ice/air interface.

Geothermal heat flows into the ice in contact with bedrock and adjust dynamically to the thermal state of the base (Aschwanden et al., 2012; Kleiner et al., 2015). The spatial pattern of the geothermal flux is taken from Greve (2005, scenario hf_pmod2). The ice surface temperature includes Dirichlet conditions from the atmospheric forcing explained above.

For all simulations, the ice front is fixed in time, and a minimum ice thickness of 10 m is applied. This implies that calving and melting exactly compensates the outflow through the margins and initially glaciated points are not allowed to become ice-free. However, regions that reach this minimum thickness ~~are assumed to retreat~~have retreated. The grounding line is allowed to evolve freely according to a sub-grid parameterization scheme, which tracks the grounding line position within the element (Seroussi et al., 2014).

Model calculations are performed on a horizontally unstructured grid with a higher resolution, $l_{\min} = 1\,\mathrm{km}$, in fast flow regions and coarser resolution, $l_{\max} = 20\,\mathrm{km}$, in the interior. The vertical ~~discretisation~~ discretization comprises 15 layers refined towards the base where vertical shearing becomes more important. The complete mesh comprises 574 056 elements. Velocity, enthalpy (i.e. temperature and microscopic water content) and geometry fields are computed on each vertex of the mesh using piecewise-linear finite elements. The Courant-Friedrichs-Lewy condition (Courant et al., 1928) dictates a time step of 0.025 years. Using the AWI cluster Cray-CS 400 computer, a simulation with an integration time of 340 years requires ≈ 8 hours on 16 nodes comprised of 36 CPUs.

2.6 Initial state

Future projections of ice sheet evolution first require the determination of the initial state. Different methods are currently used to initialize ice sheets and it has been shown, that the initial state is crucial for projections of ice dynamics (Bindschadler

et al., 2013; Nowicki et al., 2013; Goelzer et al., 2018). The recent initMIP-GrIS intercomparison effort (Goelzer et al., 2018) ~~focusses~~ focuses on the different initialization techniques applied in the ice flow modelling community and found none of them is the method of choice in terms of a good match to observations and a long term continuity. All methods are required for modelling the projections of the GrIS planned within CMIP6 phase (Nowicki et al., 2016) on time scales up to a few hundred years. However, while inverse modelling is well established for estimating basal properties, the temperature field is difficult to constrain without performing an interglacial thermal spin-up.

Here, we ~~setup~~ employ a hybrid approach between spin-up and inversion scheme to estimate the initial state. ~~The ice sheet~~ For the hybrid initialization we make the three basic simplifications: (1) The currently observed present-day elevation is taken constant for the entire glacial cycle. (2) the basal friction coefficients obtained from the inversion is taken constant for the past glacial cycle, and (3) the temperature changes from the GRIP record are applied to the whole ice sheet without spatial variations.

The ice sheet geometry (bed, ice thickness and ice sheet mask) is taken from the mass-conserving BedMachine Greenland data set v2 (Morlighem et al., 2014). The geometric input for thickness and ice sheet mask are masked to exclude glaciers and ice caps surrounding the ice sheet proper. An initial relaxation run over 50 years assuming no sliding and constant ice temperature of -20°C is performed to avoid spurious noise that arise from errors and biases in the datasets. A temperature spin-up is then performed using this time-invariant geometry. As the computational expensive BP approximation is employed, mesh refinements are made at certain points during the whole initialization procedure (see Table 3). The first mesh sequence is starting 125 kyr before ~~1990~~ present and run up to the year 1960 and assumes a spatially constant friction coefficient $k^2 = 50\,\mathrm{s\,m^{-1}}$ and forced with paleo-climatic conditions. The imposed paleo-climatic conditions is a multi-year mean from the years 1960 to 1990 of the RACMO2 product (Ettema et al., 2009) and offset by a spatially constant surface temperature anomaly for the last 125 kyr based on the GRIP surface temperature history derived from the $\Delta^{18}O$ record (Dansgaard et al., 1993). The initial ice temperature at 125 kyr before ~~1990~~ present is a steady-state temperature distribution taken from a spin-up with time independent climatic conditions from the reference period 1960–90. The spin-up is done to 1960 in order to start the projections before the critical time of Greenland's peripheral glaciers mass balance decrease (Noël et al., 2017) with an additional buffer of approx. 30 years.

In the subsequent basal-friction inversion, the ice rheology is kept constant using the enthalpy field from the end of the temperature spin-up. The inversion approach infers the basal friction coefficient k^2 in Eq. 6 by minimizing a cost function that measures the misfit between observed and ~~modelled~~ modeled horizontal velocities (Morlighem et al., 2010). Observed horizontal surface velocities are taken from (Rignot and Mouginot, 2012). The procedure of temperature spin-up and inversion is repeated on the subsequent three mesh sequences. The repeated temperature spin-ups starting 125 kyr, 25 kyr and 15 kyr before 1990 and again run up to the year 1960. The initial values for the temperature field at these times are taken from the respective times from the previous mesh sequence; the basal-friction coefficient is updated from the inversion on the previous mesh sequence. The mesh sequencing reduces the expense of initialization and produces a sufficiently consistent result in terms of velocity and enthalpy. Note that mesh sequence 1-3 are only used during initialization while the final solution of mesh sequence 4 at year 1960 of this procedure is used as initial state for all projections presented below.

Table 3. Mesh Statistics.

mesh sequence	$l_{\min}$ (km)	$l_{\max}$ (km)	number of elements	integration time in thermal spin-up (kyr)
1	15	50	117 586	125
2	5	50	192 220	125
3	2.5	35	272 650	25
4	1	20	574 056	15

~~For the hybrid initialization we make the three basic assumptions: (1) The currently observed present-day elevation is valid for the entire glacial cycle: changes in elevation and spatial extent of the GrIS are ignored, (2) the basal friction coefficient obtained from the inversion is valid for the past glacial cycle, and (3) the GRIP record can be applied to the whole ice sheet without spatial variations.~~

Please note, that similar results from this procedure have been submitted to the ISMIP6 initMIP-Greenland effort (Goelzer et al., 2018), but the simulations were run with the geothermal flux distribution by Shapiro and Ritzwoller (2004) and additionally with a time independent climate forcing representing present-day conditions. However, by using the modified heat-flux distribution by Greve (2005, scenario hf_pmod2) we found a generally better agreement to measured basal temperatures at ice core locations. Basically, the comparison of simulated to observed temperatures at the ice base shows too low temperatures for some locations. Due to the fact, that the applied inversion technique for the friction coefficient allows sliding everywhere, the portion of deformational shearing may be underestimated, which cannot be proven without any observations of basal velocities that are unfortunately ~~not existing at all~~do not exist. However, for our projections on centennial timescales this is a negligible effect (Seroussi et al., 2013).

2.7 Synthetic and dynamic surface mass balance parameterization

As we perform a one-way coupling of the climatic forcing the SMB-elevation feedback needs to be considered. Here we rely on the dynamic SMB parameterization developed by Edwards et al. (2014a, b) and previously applied by Goelzer et al. (2013). This relationship was estimated from a set of MAR simulations in which the the ice sheet surface elevation was altered. The parameterization assumes that the effect of SMB trends follow a linear relationship

$$\mathrm{SMB}_{\mathrm{dyn}}(x,y,t) = \mathrm{SMB}_{\mathrm{clim}}(x,y,t) + b_i(h_s(x,y,t) - h_{\mathrm{fix}}(x,y)), \tag{7}$$

where $\mathrm{SMB}_{\mathrm{dyn}}(x,y,t)$ and $\mathrm{SMB}_{\mathrm{fix}}(x,y,t)$ are the SMB values with and without taking height changes into account, respectively. The surface elevation changes are taken from ISSM elevation $h_s(x,y,t)$ while running the simulation and a reference elevation $h_{\mathrm{fix}}(x,y)$. In our setup the reference elevation correspond to the ISSM ice surface elevation at the initial state.

In this parameterization the SMB gradient b_i is dependent of both location and sign. It can take four values and a separation is made on the location relative to 77°N and on the sign of the SMB. This separates regions of largely different sensitivity,

namely the ablation zone with a larger gradient compared to the accumulation zone, and a more sensitive ablation zone in the South compared to the North. While a complete uncertainty analysis is given by Edwards et al. (2014a), only the maximum likelihood gradient set, $\boldsymbol{b} = (b_p^N, b_n^N, b_p^S, b_n^S)$, is used here:

$$
\begin{aligned}
b_p^N &= 0.085\,\mathrm{kg\,m^{-3}\,a^{-1}},\\
b_n^N &= 0.543\,\mathrm{kg\,m^{-3}\,a^{-1}},\\
b_p^S &= 0.063\,\mathrm{kg\,m^{-3}\,a^{-1}},\\
b_n^S &= 1.890\,\mathrm{kg\,m^{-3}\,a^{-1}},
\end{aligned}
$$

where the subscripts (p, n) and the superscripts (N, S) indicate the evaluation of the SMB sign and the region separation, respectively. Please note, that the employed relationship with their parameters may change using a setup from SEMIC.

A shortcoming of the performed hybrid initialization is, that usually a fixed initial ice sheet causes a model drift when imposing the ice thickness equation. This is a result from using an ice sheet that is not in equilibrium with the applied SMB and ice flux divergence. We utilize the local ice thickness imbalance once the ice sheet is released from its fixed topography from an one year unforced relaxation run, i.e. $\Delta\mathrm{SMB}(x, y, t) = 0$ in Eq. 5. The resulting $\partial H/\partial t$ is subtracted as a surface mass balance correction, $\mathrm{SMB_{corr}}(x, y)$, for the further runs (similar as in Price et al. (2011); Goelzer et al. (2018)). However, instead of assuming an zero SMB anomaly one could calculate the anomaly with a GCM input from the CMIP5 pre-industrial scenario. But given the small temperature changes the SMB anomaly will be close to zero and the calculated ice thickness imbalance is unlikely affected by it. However, the final SMB correction is on average 0.01 m $\mathrm{a^{-1}}$, with 5% of the total ice-sheet area having a correction of >25 m $\mathrm{a^{-1}}$, predominantly at marine-terminated ice margins and ice streams (Fig. 6). For these locations the synthetic SMB correction can be considered as an additional ice thinning or thickening from dynamic discharge that is not intrinsically simulated. A performed control run with the imposed SMB correction exhibits a ~~negligible~~ small model drift in terms of sea level equivalent (SLE, black dashed line in Fig. 11 and section 3.3).

The final surface mass balance that the numerical ice flow model sees is composed of several components

$$\mathrm{SMB} = \mathrm{SMB_{clim}}(x, y, t) - \mathrm{SMB_{corr}}(x, y) + \mathrm{SMB_{dyn}}(x, y, t)\,. \tag{8}$$

3 Results

3.1 Forcing fields

For the different GCMs used we compute ice surface temperature T_s differences between 2100/2300 and 2000 as a multi-year mean over five years do reduce the inter-annual variability (Fig. 7). HadGEM2 leads to an increase in temperatures along the northern margins by up to 4°C. By 2100 the Western areas and vast majority of the ice sheet exceed 2°C of warming. The only pronounced warming by 2300 is in the Northwestern regions, while the ice sheet surface temperatures decrease from 2100. IPSL exhibits a significantly different pattern. This simulation produces pronounced warming in the center (up to 3°C) and in the Southeast (up to 4°C) of the ice sheet, while the Northern areas are only moderately warming around 1°C during the

20th. The pattern is similar in 2300, with a moderate cooling in the West compared to 2100. The least warming is found in MIROC5, which even exhibits cooling in the southern areas by about -1°C in 2100; warming of +1°C is only reached in the North. By 2300 the entire ice sheet experiences warming; however this warming is quite moderate compared to the other two GCMs. The low magnitude of warming over Greenland compared to global warming let us infer that the mechanisms of arctic amplification is not well represented in MIROC5.

Although we do not have a measure to judge future climate warming trends, but with respect to the Arctic amplification phenomena the most plausible distribution and magnitude of surface warming is produced by HadGEM2. By contrast, MIROC5 produces less pronounced warming over Greenland that is similar to the global mean warming but exhibits a plausible pattern of warming. IPSL is spatially and temporally experiencing the largest warming; however, the distribution is not in agreement with the Arctic amplification. However, the assessment of the GCMs is in line with skill tests performed by Watterson et al. (2014) on a global scale. They assigned skill cores by comparing individual GCM output data against re-analysis data. The analysis indicates that all 25 models have a substantial degree of skill, however, HadGEM2 is ranked in the top, MIROC5 in the middle, and IPSL in lower part.

Figure 8 presents in a similar fashion as Fig. 7 the differences in SMB between 2100/2300 and 2000 as a multi-year mean over five years each. The difference in SMB 2100-2000 of SEMIC-HadGEM2 indicates a similar pattern as presented by Krapp et al. (2017) using MAR (Fettweis et al., 2013). Increasing SMB in the eastern part of the ice sheet with a maximum in the southern half of the ice sheet; at the ice sheet margins ablation is increased. The same pattern is characteristic for 2300-2000, but with slightly decrease of melting and accumulation. The SMB is reduced in the center, leaving a wide area with differences in SMB of 0.5 m a^{-1} and less. The SMB difference of SEMIC-IPSL is showing a similar pattern with enhanced amplitudes compared to SEMIC-HadGEM2, in particular, an the southwestern margin; melting in the Southwest is increased up to 1 m a^{-1}. In contrast a SMB gain is concentrated in the center-East by 2300. The most astonishing result is the ΔSMB pattern in SEMIC-MIROC5. Increasing SMB along the southwestern and southern margins in contrast to gently decreasing SMB in the center of the ice sheet. By 2300 ΔSMB the pattern changes slightly and SMB is decreasing in the southwestern margins. The magnitude of ΔSMB is less compared to SEMIC-HadGEM2 and SEMIC-IPSL.

3.2 Present day elevation and velocities

Figure 9 displays exemplary the observed and simulated velocities for the year 2000 (defined here as present day) after a period of forcing with ~~HadGEM2-ES~~ SEMIC-HadGEM2 from 1960 onwards. The resulting horizontal velocity field captures all major features well, including the North East Greenland Ice Stream (NEGIS). Outlet glaciers terminating in narrow fjords in the southeastern region are resolved, however, slow moving areas tend to retreat below minimum ice thickness and with that the ice extent in this area is underestimated. However, ice surface elevations agree fairly well (Fig. 10~~a~~b). In general large outlet glaciers like Kangerdlusuaq, Helheim and Jakobshavn Isbræ reveal lower velocities in their fast termini that reflects the high RMS of about ~~390~~400 m a^{-1} (Fig. 10~~b). Compared to the low RMS values of <20 m a^{-1} for the AWI-ISSM results on the regular 5 km grid given in Goelzer et al. (2018), the~~ a). The RMS analysis here was done on the ~~original~~ native grid with the

high resolution in fast flow regions and ~~on other hand~~ the model was already run 40 years forward in time. Compared to this values, the AWI-ISSM results on the regular 5 km grid given in Goelzer et al. (2018) have a lower RMS value of $<20\,\mathrm{m\,a^{-1}}$.

3.3 Projections of mass change

After passing the assumed critical time of ~~decreasing SMB of~~ declining SMB of the GrIS and the present day state, the ice sheet experienced a warming and associated mass loss from surface mass balance. Projections of the evolution of SLE of the ice sheet under RCP2.6 scenario ~~with overshoot~~ until 2100 and 2300 are shown in Fig. 11 for each GCM (~~straight~~ solid lines) and Table 4. The simulated volume above floatation is converted into the total amount of global sea level equivalent (SLE) by assuming an ocean area of about $3.618\times10^8\,\mathrm{km^2}$. Although the control run shows a ~~negligible~~ small model drift in terms of SLE ~~,~~ (-1.4 and -0.7 mm for 2100 and 2300, respectively), the RCP2.6 projected SLE is corrected by the control run. By 2100, the model range of Greenland sea-level contributions is between 21.3 and 38.1 mm with an average of 27.9 mm and by 2300 between 36.2 and 85.1 mm with ~~and~~ an average of 53.7 mm. Compared to Fürst et al. (2015) our mean values are lower but still in their model ~~variability~~range.

The evolution of the mass change, expressed as sea level equivalent, (Fig 11) is showing distinct ~~behaviours~~behaviors: between 1960–2000 almost no change for ~~HadGEM2-ES and IPSL-CM5A-LR while MIROC5~~ SEMIC-HadGEM2 and SEMIC-IPSL while SEMIC-MIROC5 is gaining mass; a change in trend with a minor increase between 2000–2015 and a steep increase from then on for ~~HadGEM2-ES and IPSL-CM5A-LR~~SEMIC-HadGEM2 and SEMIC-IPSL; SLE increase for ~~MIROC5~~ SEMIC-MIROC5 is more gently. The steep rise in SLE for ~~HadGEM2-ES and IPSL-CM5A-LR~~ SEMIC-HadGEM2 and SEMIC-IPSL is linked to the steep reduction in SMB for both models at the same time. The kink of SLE in ~~HadGEM2-ES and IPSL-CM5A-LR~~ SEMIC-HadGEM2 and SEMIC-IPSL around 2050 is caused by a positive SMB anomaly (compare Fig. 4). Also ~~MIROC5 represents~~ SEMIC-MIROC5 shows this peak in SMB, however slightly later, around 2060. These short-term drops in SLE are linked to positive anomalies in SMB. For ~~HadGEM2-ES~~ SEMIC-HadGEM2 the ice sheet contribution until 2300 generally increases continuously while for ~~IPSL-CM5A-LR and MIROC5~~ SEMIC-IPSL and SEMIC-MIROC5 the increase levels off. This is an intriguing effect as ~~HadGEM2-ES and IPSL-CM5A-LR~~ SEMIC-HadGEM2 and IPSL are showing in terms of warming over GrIS a similar ~~behaviour~~ behavior (Fig. 1). In fact, the SMB of ~~IPSL-CM5A-LR~~ SEMIC-IPSL recovers from 2050 onwards (Fig. 4), while the SMB of ~~HadGEM2-ES~~ SEMIC-HadGEM2 remains on a low level.

For the RCP2.6 scenario without overshoot the ~~behaviour~~ behavior of SLE for ~~HadGME2-ES~~ SEMIC-HadGME2 is similar but with lower values. The SLE for ~~MIROC5~~ SEMIC-MIROC5 is by 2100 approx. 5 mm lower but approaches the same value at 2300 without attaining a pronounced plateau. A striking feature is the much lower SLE estimated from ~~IPSL-CM5A-LR~~ SEMIC-IPSL which never exceeds a value of 10 mm and gains mass about 2225 onwards. The average SLE from all three GCMs is 17.4 mm by 2100 and 37.1 mm by 2300, that is approximately one third less compared to the RCP2.6 scenario~~with overshoot~~.

The observed sea level contribution between 2002 and 2014 is $0.73\,\mathrm{mm\,a^{-1}}$ (Rietbroek et al., 2016). In the same period the simulated contribution is only $0.16\,\mathrm{mm\,a^{-1}}$ for ~~HadGEM2-ES~~SEMIC-HadGEM2, $0.17\,\mathrm{mm\,a^{-1}}$ for ~~IPSL-CM5A-LR~~ SEMIC-IPSL and lowest for ~~MIROC5~~ SEMIC-MIROC5 with $0.13\,\mathrm{mm\,a^{-1}}$. In order to assess a potential temporal lag be-

Table 4. Contribution of the Greenland ice sheet to global sea-level change by 2100 and 2300 in mm SLE under RCP2.6 scenario with and without overshoot.

Model / Study	2100		2300	
	with overshoot	without overshoot	with overshoot	without overshoot
~~HadGEM2-ES~~ SEMIC-HadGEM2	38.1	29.6	85.1	66.9
~~IPSL-CM5A-LR~~ SEMIC-IPSL	24.4	7.5	36.2	3.4
~~MIROC5~~ SEMIC-MIROC5	21.3	15.0	39.9	40.9
Average	27.9	17.4	53.7	37.1
Fürst et al. (2015)	42.3±18.0	-	88.2±44.8	-

tween simulated and observed value, mean values of similar periods are calculated (Fig. 5). None of the models reach the observed value ~~; HadGEM2-ES~~ (solid black line in Fig. 5); HadGEM2 reaches a maximum value of 0.59 mm a^{-1} 13 years later; ~~IPSL-CM5A-LR~~ SEMIC-IPSL a value of 0.48 mm a^{-1} 12 years later and ~~MIROC5~~ SEMIC-MIROC5 a value of 0.36 mm a^{-1} 40 years later. For the RCP2.6 scenario without overshoot, the values are smaller. Since a future ocean forcing and calving front retreat is not considered here, the response of the ice sheet is likely underestimated. Comparing the sea level contributions of each SEMIC-GCM to the sea level contribution of 0.4 mm a^{-1} calculated from RACMO2.3 for the same period (dashed black line in Fig. 5) reveals a better agreement. SEMIC-HadGEM2 reaches this value 8 years later for RCP2.6 scenario with overshoot and 9 years later for the RCP2.6 scenario without overshoot; SEMIC-IPSL reaches this value 10 years later for RCP2.6 with overshoot.

3.4 ~~Future climatic forcing fields~~

~~For the different GCMs used we compute ice surface temperature T_s differences between 2100/2300 and 2000 as a multi-year mean over five years do reduce the inter-annual variability (Fig. 7). HadGEM2-ES leads to an increase in temperatures along the northern margins by up to 4°C. By 2100 the Western areas and vast majority of the ice sheet exceed 2°C of warming. The only pronounced warming by 2300 is in the Northwestern regions, while the ice sheet surface temperatures decrease from 2100. IPSL-CM5A-LR exhibits a significantly different pattern. This simulation produces pronounced warming in the center (up to 3°C) and in the Southeast (up to 4°C) of the ice sheet, while the Northern areas are only moderately warming around 1°C during the 20th. The pattern is similar in 2300, with a cooling in the West. The cooling after 2100 is by far less than in HadGEM2-ES. The least warming is found in MIROC5, which even exhibits cooling in the southern areas by about -1°C and +1°C is only reached in 2100 in the North. By 2300 the entire ice sheet experiences warming; however this warming is quite moderate compared to the other two GCMs. The low magnitude of warming compared to global warming let us infer that the mechanisms of arctic amplification is not well represented in MIROC5.~~

~~Although we do not have a measure to judge future climate warming trends, but with respect to the Arctic amplification phenomena the most plausible distribution of surface warming is produced by HadGEM2-ES and MIROC5, while only~~

HadGEM2-ES also reaching a plausible magnitude of warming with overshooting the global mean values. IPSL-CM5A-LR is spatially and temporally experiencing the largest warming; however, the distribution is not in agreement with the Arctic amplification. However, the assessment of the GCMs is in line with skill tests performed by Watterson et al. (2014). They assigned skill cores by comparing individual GCM output data against re-analysis data. The analysis indicates that all 25 models have a substantial degree of skill, however, HadGEM2-ES is ranked in the top, MIROC5 in the middle, and IPSL-CM5A-LR in lower part.

Figure 8 presents in a similar fashion as Fig. 7 the differences in SMB between 2100/2300 and 2000 as multi-year mean over five years each. The difference in SMB 2100-2000 of HadGEM2-ES indicates a similar pattern presented by Krapp et al. (2017) using MAR (Fettweis et al., 2013). Increasing SMB in the eastern part of the ice sheet with a maximum in the southern half of the ice sheet; at the ice sheet margins ablation is increased. The same pattern is characteristic for 2300-2000, but with a further increase of melting and decrease of accumulation in the center of the ice sheet. The SMB is reduced in the center, leaving a wide area with differences in SMB of 0.5 m a^{-1} and more, except for the ablation at the ice sheet margin. Moreover, most evident is a decreasing SMB in the Northeast. The SMB difference of IPSL-CM5A-LR is showing a similar pattern with enhanced amplitudes compared to HadGEM2-ES, in particular, an the southwestern margin; melting in the Southwest is increased up to 1 m a^{-1}. In contrast a SMB gain is concentrated in the center-East and Northwest by 2300; the margin in the northwest is experiencing a SMB increase of +1 m a^{-1}. The most astonishing result is the ΔSMB pattern in MIROC5. Increasing SMB along the southwestern and southern margins in contrast to gently decreasing SMB in the center of the ice sheet. By 2300 ΔSMB the pattern changes and SMB is generally increasing in the East and decreasing at the western margins; the magnitude of ΔSMB is less compared to HadGEM2-ES and IPSL-CM5A-LR.

3.4 Ice thickness change and dynamic response

Extensive marginal thinning is experienced by forcing the ice sheet with HadGEM2-ES and IPSL-CM5A-LR SEMIC-HadGEM2 and SEMIC-IPSL (Fig. 13). In contrast to the mass loss near the margin the interior shows increased thickening; IPSL-CM5A-LR thickening; IPSL reveals more thickening in the interior. Generally the pattern large-scale pattern of marginal thinning and central thickening correlates with observations (Helm et al., 2014) except that Petermann and Kangerdlusuaq glaciers shows show an opposite trend. With a forcing of MIROC5 the pattern of the elevation change is different with thinning in the southern center of the ice sheet; the northern center experienced thickening. Although thinning occurs at the margin it is less extensive compared to the other GCMs. The ice tongue 79°N Glacier is in all forcings threatened in their existence, even with the moderate forcing of MIROC5.

The response of ice velocities to RCP2.6 forcing is presented in Fig. 14, where the change in horizontal surface velocities is shown for all scenarios as a difference between 2100–2000 and 2300–2000 (each as five year mean). For all GCM SEMIC-GCM forcings the ice response shows relatively the same behaviourbehavior. The NEGIS, Jakobshavn Isbræ, Helheim, Ryder glaciers and Hagen Bræ experience acceleration; deceleration is present at Petermann and Kangerdlusuaq glaciers. However, the magnitude of response is among all models different. Most prominent at the western margin where HadGEM2-ES lead SEMIC-HadGEM2 lead to the strongest acceleration while MIROC5 SEMIC-MIROC5 to the lowest. Though, the acceleration

~~of Jakobshavn Isbræis present in our simulations, however, not to the extent of the observations (Joughin et al., 2014). This is due to the lack of forcing with calving rates in our simulations, which has been key for reproducing the observed acceleration and retreat in Bondzio et al. (2017).~~

4 Discussion

Fürst et al. (2015) performed a comprehensive ensemble study for a suite of 10 GCMs (HadGEM2-ES, IPSL-CM5A-LR and MIROC5 included) and four different RCP scenarios. For the RCP2.6 scenario they estimate an abated sea level contribution of 42.3±18.0 mm by 2100 and 88.2±44.8 mm by 2300. Our averaged result of a sea level contribution under RCP2.6 forcing is slightly lower but still in their ensemble variability. The resultant projection by Fürst et al. (2015) included contributions from lubrication, marine melt and SMB-coupling while ours ~~account~~ accounts for SMB forcing only. The lubrication effect was diagnosed to have a negligible effect on the overall mass budget, but the oceanic influence on the total ice loss explains about half of the mass loss for RCP2.6. Since a future ocean forcing and calving front retreat is not considered here, the response of the ice sheet is likely underestimated here. By 2010 the cumulative ice discharge ~~for HadGEM2-ES~~ anomaly for SEMIC-HadGEM2 contributes with about 15% to the ice loss. By 2100 and 2300 the contribution is below 3 and 7%, respectively and becomes negligible. For ~~IPSL-CM5A-LR and MIROC5~~ SEMIC-IPSL and SEMIC-MIROC5 the cumulative effect of ice discharge anomaly shares less than 10% of the total mass budget by 2010 and 2100 but increases towards 17% by 2300. The different ~~behaviour~~ behavior can be explained by the interaction with the SMB and ice dynamics as the relative importance of outlet glacier dynamics decreases with increasing surface melt (Goelzer et al., 2013; Fürst et al., 2015). Increased ice discharge causes dynamic thinning further upstream, lowering of the ice surface and thereby intensifies surface melting due to the associated warming of the near surface. Surface melting in turn competes with the discharge increase by removing ice before it reaches the marine margin. The simulated increase of ice discharge for ~~IPSL-CM5A-LR and MIROC5~~ SEMIC-IPSL and SEMIC-MIROC5 is therefore linked to the recovery of SMB of the course of the 22$^{\text{nd}}$ century. Still, the SMB remains the dominant factor for mass loss. The speed-up observed from all scenarios merely ~~transport~~ transports ice form the interior but is melted before it reaches the ice sheet margin. However, the values for sea level contribution of this study may serve as a lower bound, as processes (ocean forcing and calving) proven to play a major role in GrIS mass loss are not yet represented by the model.

Additionally, the calculation of the surface mass balance are based on different methods. Fürst et al. (2015) rely on the rather simple and empirical derived PDD scheme, while we use an more advanced energy-balance approach. So far the sensitivity of melting to warming of these class of models is not well understood. Comparisons of PDD models and energy-balance models suggested that the former are too sensitive to climate change and produce a larger runoff response (van de Wal, 1996; Bougamont et al., 2007; Graversen et al., 2011). On the other hand Goelzer et al. (2013) attempted to make a robust comparison and find that a PDD model underestimates sea level rise by 14–31% compared to MAR. An Assessment of the SMB and its impact on sea level contribution calculated by the PDD scheme in Fürst et al. (2015) and the SEMIC model from this study cannot be drawn, because of the strong interaction between ice loss, ice dynamics and external forcings. As the cumulative

discharge rates in the mass budget are higher compared to Fürst et al. (2015), this may indicate a lower SMB forcing. However, compared to other models that participate in the initMIP-GrIS exercise (Goelzer et al., 2018), our setup is whether on the higher end nor of the lower spectrum of estimated mass loss. Additionally, we have conducted SeaRISE experiments similar to Bindschadler et al. (2013), which showed us that we are within the spread among the models, in particular, for the amplified climatic scenarios C1, C2, and C3 (not shown here).

The modified RCP2.6 scenario without overshoot projected a sea level contribution that is on average about 38% and 31% less by 2100 and by 2300, respectively. For ~~HadGEM2-ES and MIROC5~~ SEMIC-HadGEM2 and SEMIC-MIROC5 the partition of the mass budget is relatively similar to the ~~scenario with overshoot~~ RCP2.6 scenario but with a slightly increased cumulative discharge ~~. For IPSL-CM5A-LR the behaviour~~ anomaly. For SEMIC-IPSL the behavior is more irregular ~~. It~~ and gains mass during the last century, as a result from an increasing SMB which is partly compensated by enhanced ice discharge up to 40%. However, the spread of sea level contribution is much larger compared to the RCP2.6 scenario~~with overshoot~~. In particular, in 2300 the range of sea level contribution is between 3.4–66.9 mm. The very low estimated contribution of 3.4 mm is a result from the ~~IPSL-CM5A-LR~~ SEMIC-IPSL forcing that predicts a relatively high SMB of 364 Gt yr^{-1} for the characteristic time of overshooting 1.5°C (Column '1.5°C reached' in Tab. 2). The SMB is close to present-day and therefore ~~IPSL-CM5A-LR~~ SEMIC-IPSL maintains a geometry close to present day. In contrast, SEMIC-HadGEM2 has declined to 170 Gt yr^{-1} and SEMIC-MIROC5 to 288 Gt yr^{-1}. The prolongation of these scenarios were done by repeating the forcing from a time window that reveals a stabilized climate. Repeating the last 30-year forcing field window before the characteristic time is not reasonable, because the change in warming is strongest during that period and a stabilized climate would not be reached. In fact, we would generate a non-mitigation pathway scenario with constant warming rates that will have larger melt and therefore ~~likely~~ contributes more to sea level contribution (not shown here).

The generally abated sea level contribution ~~confirms~~ is in agreement with the inferred threshold in global mean temperature before irreversible ice sheet topography changes occur. The simplified assumption behind these threshold is an integrated SMB over the whole ice sheet that becomes negative (Gregory and Huybrechts, 2006). Fettweis et al. (2013) reported a threshold of 3.5°C relative to pre-industrial, which is never exceeded under the RCP2.6 scenario. Assuming a steady state ice-sheet SMB of 400 Gt yr^{-1} ~~the~~ within the reference period the decline in SMB must be larger than -400 Gt yr^{-1} to get a continuous retreating ice sheet margin. If the mean SMB of the GrIS remains positive a new steady state ice sheet geometry may be possible, but require a balancing with the ice outflow.

At last we want to discuss if studying RCP2.6 allows to draw significant conclusions on the development of sea level rise due to mass loss in Greenland. We found that only a fraction of the current observed mass loss in the first two decades is represented by the model in RCP2.6. This can be attributed to different factors: the current emissions are above the RCP2.6 limit and hence the natural system evolves on a different route than RCP2.6. Secondly, the three GCMs are quite different in response to the RCP2.6 forcing and ~~last but not least, the model~~ the ISM used itself does not represent all mechanisms, in particular the lack of oceanic forcing is causing a reduced sea level rise. Hence, a new emission scenario, that represent the real RCP pathway in the recent past, would be most useful for future studies like ours.

5 Conclusions

We have applied climate forcings based on the low-emission scenario CMIP5 RCP2.6 of three underlying GCMs (HadGEM2-ES, IPSL-CM5A-LR, MIROC5) to ISSM. Despite all three GCMs are based on RCP2.6, their temperature variation – globally and regionally for GrIS – is considerably large. Arctic amplification causes a near-surface air temperature increase over Greenland by a factor of ≈ 2.4 and 2 in HadGEM2-ES and IPSL-CM5A-LR, respectively. MIROC5 reveals nearly no arctic amplification. In order to force the ice sheet model with a reliable SMB, a physically based surface energy balance model of of intermediate complexity (SEMIC) was applied. The estimated sea level contribution for the RCP2.6 peak and decline scenario is ranging in our simulations from 21–38 mm by 2100 and 36–85 mm by 2300 and are up to 30–40% higher compared to a scenario without overshoot. Despite the reduced SMB is the warmer climate, a future steady-state ice sheet with lower surface and volume might be possible.

Although the thickness change pattern agrees well with observations and acceleration of NEGIS, Helheim Glacier and Jakobshavn Isbræ is captured in our simulations, the estimated sea level contribution is potentially underestimated due to the following drawbacks of our study: (i) retreat of glaciers due to oceanic forcing (melt at vertical cliffs and/or calving rates) and (ii) seasonality due to lubrication arising from supra-glacial melt water is not included. This leads to the conclusion that the projections may serve as a lower bound of the contribution of Greenland to sea level rise under RCP2.6 climate scenario. This limits also the advantageous treatment of the physics in our model setup, meaning that all the benefits from a high-resolution higher order model are not yet contributing to the extent they potentially could. Our results further indicate, that uncertainties stem from the underlying climate model to calculate the surface mass balance.

Code availability. The ice sheet model ISSM is available at issm.jpl.nasa.gov and not distributed by the authors of this manuscript. SEMIC is available from https://gitlab.pik-potsdam.de/krapp/semic-project and not distributed by the authors of this manuscript.

Author contributions. M.R. conducted ISSM simulations, coupled SEMIC output to ISSM. M.R. and A.H. designed the study, analyzed the results and wrote major parts of the manuscript. K.F. and S.L. selected, prepared and contributed GCM forcings. U.F. has contributed advice on the albedo scheme and checked the GCM input data.

Competing interests. There are no competing interests present.

Acknowledgements. This work was funded by BMBF under grant EP-GrIS (01LS1603A) and the Helmholtz Alliance Climate Initiative (REKLIM). We would like to thank ~~both reviewers~~ an anonymous reviewer and Clemens Schannwell for the detailed review containing many helpful remarks and constructive criticism that helps to improve the manuscript. We acknowledge the technical support given by Mario

Krapp (PIK) with SEMIC. We are grateful for the NetCDF interface to SEMIC provided by Paul Gierz (AWI). We would like to thank Vadym Aizinger, Natalja Rakowsky and Malte Thoma for maintaining excellent computing facilities at AWI. We also enthusiastically acknowledge the general support of the ISSM team.

References

Aschwanden, A., Bueler, E., Khroulev, C., and Blatter, H.: An enthalpy formulation for glaciers and ice sheets, Journal of Glaciology, 58, 441–457, https://doi.org/10.3189/2012JoG11J088, 2012.

Bauer, E. and Ganopolski, A.: Comparison of surface mass balance of ice sheets simulated by positive-degree-day method and energy balance approach, Climate of the Past, 13, 819, 2017.

Beckmann, A. and Goosse, H.: A parameterization of ice shelf–ocean interaction for climate models, Ocean Modelling, 5, 157–170, https://doi.org/10.1016/S1463-5003(02)00019-7, 2003.

Bindschadler, R. A., Nowicki, S., Abe-Ouchi, A., Aschwanden, A., Choi, H., Fastook, J., Granzow, G., Greve, R., Gutowski, G., Herzfeld, U., Jackson, C., Johnson, J., Khroulev, C., Levermann, A., Lipscomb, W. H., Martin, M. A., Morlighem, M., Parizek, B. R., Pollard, D., Price, S. F., Ren, D., Saito, F., Sato, T., Seddik, H., Seroussi, H., Takahashi, K., Walker, R., and Wang, W. L.: Ice-sheet model sensitivities to environmental forcing and their use in projecting future sea level (the SeaRISE project), Journal of Glaciology, 59, 195–224, https://doi.org/doi:10.3189/2013JoG12J125, 2013.

Blatter, H.: Velocity and stress fields in grounded glaciers: a simple algorithm for including deviatoric stress gradients, Journal of Glaciology, 41, 333–344, 1995.

Bondzio, J. H., Seroussi, H., Morlighem, M., Kleiner, T., Rückamp, M., Humbert, A., and Larour, E. Y.: Modelling calving front dynamics using a level-set method: application to Jakobshavn Isbræ, West Greenland, The Cryosphere, 10, 497–510, https://doi.org/10.5194/tc-10-497-2016, 2016.

Bondzio, J. H., Morlighem, M., Seroussi, H., Kleiner, T., Rückamp, M., Mouginot, J., Moon, T., Larour, E. Y., and Humbert, A.: The mechanisms behind Jakobshavn Isbræ's acceleration and mass loss: A 3-D thermomechanical model study, Geophysical Research Letters, 44, 6252–6260, https://doi.org/10.1002/2017GL073309, 2017GL073309, 2017.

Bougamont, M., Bamber, J. L., Ridley, J. K., Gladstone, R. M., Greuell, W., Hanna, E., Payne, A. J., and Rutt, I.: Impact of model physics on estimating the surface mass balance of the Greenland ice sheet, Geophysical Research Letters, 34, https://doi.org/10.1029/2007GL030700, 2007.

Choi, Y., Morlighem, M., Rignot, E., Mouginot, J., and Wood, M.: Modeling the Response of Nioghalvfjerdsfjorden and Zachariae Isstrøm Glaciers, Greenland, to Ocean Forcing Over the Next Century, Geophysical Research Letters, 44, 11,071–11,079, https://doi.org/10.1002/2017GL075174.

Courant, R., Friedrichs, K., and Lewy, H.: Über die Partiellen Differenzengleichungen der Mathematischen Physik, Mathematische Annalen, 100, 32–74, 1928.

Dansgaard, W., Johnsen, S., Clausen, H., Dahl-Jensen, D., Gundestrup, N., Hammer, C., Hvidberg, C., Steffensen, J., Sveinbjörndottir, A., Jouzel, J., and Bond, G.: Evidence for general instability of past climate from a 250-kyr ice-core record, Nature, 364, 218–220, https://doi.org/doi:10.1038/364218a0, 1993.

Edwards, T. L., Fettweis, X., Gagliardini, O., Gillet-Chaulet, F., Goelzer, H., Gregory, J. M., Hoffman, M., Huybrechts, P., Payne, A. J., Perego, M., Price, S., Quiquet, A., and Ritz, C.: Probabilistic parameterisation of the surface mass balance elevation feedback in regional climate model simulations of the Greenland ice sheet, The Cryosphere, 8, 181–194, https://doi.org/10.5194/tc-8-181-2014, 2014a.

Edwards, T. L., Fettweis, X., Gagliardini, O., Gillet-Chaulet, F., Goelzer, H., Gregory, J. M., Hoffman, M., Huybrechts, P., Payne, A. J., Perego, M., Price, S., Quiquet, A., and Ritz, C.: Effect of uncertainty in surface mass balance elevation feedback on projections of the future sea level contribution of the Greenland ice sheet, The Cryosphere, 8, 195–208, https://doi.org/10.5194/tc-8-195-2014, 2014b.

Erokhina, O., Rogozhina, I., Prange, M., Bakker, P., Bernales, J., Paul, A., and Schulz, M.: Dependence of slope lapse rate over the Greenland ice sheet on background climate, Journal of Glaciology, 63, 568, https://doi.org/10.1017/jog.2017.10, 2017.

Ettema, J., van den Broeke, M. R., van Meijgaard, E., van de Berg, W. J., Bamber, J. L., Box, J. E., and Bales, R. C.: Higher surface mass balance of the Greenland ice sheet revealed by high-resolution climate modeling, Geophysical Research Letters, 36, n/a–n/a, https://doi.org/10.1029/2009GL038110, l12501, 2009.

Fettweis, X., Franco, B., Tedesco, M., van Angelen, J. H., Lenaerts, J. T. M., van den Broeke, M. R., and Gallée, H.: Estimating the Greenland ice sheet surface mass balance contribution to future sea level rise using the regional atmospheric climate model MAR, The Cryosphere, 7, 469–489, https://doi.org/10.5194/tc-7-469-2013, 2013.

Fettweis, X., Box, J. E., Agosta, C., Amory, C., Kittel, C., Lang, C., van As, D., Machguth, H., and Gallée, H.: Reconstructions of the 1900–2015 Greenland ice sheet surface mass balance using the regional climate MAR model, The Cryosphere, 11, 1015–1033, https://doi.org/10.5194/tc-11-1015-2017, https://www.the-cryosphere.net/11/1015/2017/, 2017.

Frieler, K., Lange, S., Piontek, F., Reyer, C. P. O., Schewe, J., Warszawski, L., Zhao, F., Chini, L., Denvil, S., Emanuel, K., Geiger, T., Halladay, K., Hurtt, G., Mengel, M., Murakami, D., Ostberg, S., Popp, A., Riva, R., Stevanovic, M., Suzuki, T., Volkholz, J., Burke, E., Ciais, P., Ebi, K., Eddy, T. D., Elliott, J., Galbraith, E., Gosling, S. N., Hattermann, F., Hickler, T., Hinkel, J., Hof, C., Huber, V., Jägermeyr, J., Krysanova, V., Marcé, R., Müller Schmied, H., Mouratiadou, I., Pierson, D., Tittensor, D. P., Vautard, R., van Vliet, M., Biber, M. F., Betts, R. A., Bodirsky, B. L., Deryng, D., Frolking, S., Jones, C. D., Lotze, H. K., Lotze-Campen, H., Sahajpal, R., Thonicke, K., Tian, H., and Yamagata, Y.: Assessing the impacts of 1.5 °C global warming – simulation protocol of the Inter-Sectoral Impact Model Intercomparison Project (ISIMIP2b), Geoscientific Model Development, 10, 4321–4345, https://doi.org/10.5194/gmd-10-4321-2017, https://www.geosci-model-dev.net/10/4321/2017/, 2017.

Fürst, J. J., Goelzer, H., and Huybrechts, P.: Ice-dynamic projections of the Greenland ice sheet in response to atmospheric and oceanic warming, The Cryosphere, 9, 1039–1062, https://doi.org/10.5194/tc-9-1039-2015, https://www.the-cryosphere.net/9/1039/2015/, 2015.

Gill, A. E.: Atmosphere-Ocean dynamics (International Geophysics Series), academic press, 1982.

GISTEMP Team: GISS Surface Temperature Analysis (GISTEMP), NASA Goddard Institute for Space Studies. Dataset accessed 2018-04-25 at https://data.giss.nasa.gov/gistemp/, 2018.

Goelzer, H., Huybrechts, P., Fürst, J., Nick, F., Andersen, M., Edwards, T., Fettweis, X., Payne, A., and Shannon, S.: Sensitivity of Greenland Ice Sheet Projections to Model Formulations, Journal of Glaciology, 59, 733–749, https://doi.org/10.3189/2013JoG12J182, 2013.

Goelzer, H., Nowicki, S., Edwards, T., Beckley, M., Abe-Ouchi, A., Aschwanden, A., Calov, R., Gagliardini, O., Gillet-Chaulet, F., Golledge, N. R., Gregory, J., Greve, R., Humbert, A., Huybrechts, P., Kennedy, J. H., Larour, E., Lipscomb, W. H., Le clec'h, S., Lee, V., Morlighem, M., Pattyn, F., Payne, A. J., Rodehacke, C., Rückamp, M., Saito, F., Schlegel, N., Seroussi, H., Shepherd, A., Sun, S., van de Wal, R., and Ziemen, F. A.: Design and results of the ice sheet model initialisation experiments initMIP-Greenland: an ISMIP6 intercomparison, The Cryosphere, 12, 1433–1460, https://doi.org/10.5194/tc-12-1433-2018, 2018.

Graversen, R. G., Drijfhout, S., Hazeleger, W., van de Wal, R., Bintanja, R., and Helsen, M.: Greenland's contribution to global sea-level rise by the end of the 21st century, Climate Dynamics, 37, 1427–1442, https://doi.org/10.1007/s00382-010-0918-8, 2011.

Gregory, J. and Huybrechts, P.: Ice-sheet contributions to future sea-level change, Philosophical Transactions of the Royal Society of London A: Mathematical, Physical and Engineering Sciences, 364, 1709–1732, https://doi.org/10.1098/rsta.2006.1796, http://rsta.royalsocietypublishing.org/content/364/1844/1709, 2006.

Greve, R.: Relation of measured basal temperatures and the spatial distribution of the geothermal heat flux for the Greenland ice sheet, Annals of Glaciology, 42, 424–432, 2005.

Helm, V., Humbert, A., and Miller, H.: Elevation and elevation change of Greenland and Antarctica derived from CryoSat-2, The Cryosphere, 8, 1539–1559, https://doi.org/10.5194/tc-8-1539-2014, 2014.

Huybrechts, P., Letreguilly, A., and Reeh, N.: The Greenland ice sheet and greenhouse warming, Palaeogeography, Palaeoclimatology, Palaeoecology, 89, 399 – 412, https://doi.org/https://doi.org/10.1016/0031-0182(91)90174-P, http://www.sciencedirect.com/science/article/pii/003101829190174P, 1991.

IPCC: Climate Change 2013: The Physical Science Basis. Contribution of Working Group I to the Fifth Assessment Report of the Intergovernmental Panel on Climate Change, Cambridge University Press, Cambridge, United Kingdom and New York, NY, USA, https://doi.org/10.1017/CBO9781107415324, www.climatechange2013.org, 2013.

Joughin, I., Smith, B. E., Shean, D. E., and Floricioiu, D.: Brief Communication: Further summer speedup of Jakobshavn Isbræ, The Cryosphere, 8, 209–214, https://doi.org/10.5194/tc-8-209-2014, https://www.the-cryosphere.net/8/209/2014/, 2014.

Kleiner, T., Rückamp, M., Bondzio, J. H., and Humbert, A.: Enthalpy benchmark experiments for numerical ice sheet models, The Cryosphere, 9, 217–228, https://doi.org/10.5194/tc-9-217-2015, 2015.

Krapp, M., Robinson, A., and Ganopolski, A.: SEMIC: an efficient surface energy and mass balance model applied to the Greenland ice sheet, The Cryosphere, 11, 1519–1535, https://doi.org/10.5194/tc-11-1519-2017, 2017.

Lange, S.: Bias correction of surface downwelling longwave and shortwave radiation for the EWEMBI dataset, Earth System Dynamics Discussions, 2017, 1–30, https://doi.org/10.5194/esd-2017-81, https://www.earth-syst-dynam-discuss.net/esd-2017-81/, 2017.

Larour, E., Seroussi, H., Morlighem, M., and Rignot, E.: Continental scale, high order, high spatial resolution, ice sheet modeling using the Ice Sheet System Model (ISSM), Journal of Geophysical Research: Earth Surface, 117, https://doi.org/10.1029/2011JF002140, 2012.

Meinshausen, M., Smith, S. J., Calvin, K., Daniel, J. S., Kainuma, M. L. T., Lamarque, J.-F., Matsumoto, K., Montzka, S. A., Raper, S. C. B., Riahi, K., Thomson, A., Velders, G. J. M., and van Vuuren, D. P.: The RCP greenhouse gas concentrations and their extensions from 1765 to 2300, Climatic Change, 109, 213, https://doi.org/10.1007/s10584-011-0156-z, https://doi.org/10.1007/s10584-011-0156-z, 2011.

Morlighem, M., Rignot, E., Seroussi, H., Larour, E., Dhia, H. B., and Aubry, D.: Spatial patterns of basal drag inferred using control methods from a full-Stokes and simpler models for Pine Island Glacier, West Antarctica, Geophysical Research Letters, 37, https://doi.org/10.1029/2010GL043853, https://agupubs.onlinelibrary.wiley.com/doi/abs/10.1029/2010GL043853, 2010.

Morlighem, M., Rignot, E., Mouginot, J., Seroussi, H., and Larour, E.: Deeply incised submarine glacial valleys beneath the Greenland ice sheet, Nature Geoscience, 7, 418–422, https://doi.org/10.1038/ngeo2167, 2014.

Morlighem, M., Bondzio, J., Seroussi, H., Rignot, E., Larour, E., Humbert, A., and Rebuffi, S.: Modeling of Store Gletscher's calving dynamics, West Greenland, in response to ocean thermal forcing, Geophysical Research Letters, 43, 2659–2666, https://doi.org/10.1002/2016GL067695, 2016GL067695, 2016.

Moss, R. H., Edmonds, J. A., Hibbard, K. A., Manning, M. R., Rose, S. K., van Vuuren, D. P., Carter, T. R., Emori, S., Kainuma, M., Kram, T., Meehl, G. A., Mitchell, J. F. B., Nakicenovic, N., Riahi, K., Smith, S. J., Stouffer, R. J., Thomson, A. M., Weyant, J. P., and Wilbanks, T. J.: The next generation of scenarios for climate change research and assessment, Nature, 463, 747–756, http://dx.doi.org/10.1038/nature08823, 2010.

Nerem, R. S., Beckley, B. D., Fasullo, J. T., Hamlington, B. D., Masters, D., and Mitchum, G. T.: Climate-change–driven accelerated sea-level rise detected in the altimeter era, Proceedings of the National Academy of Sciences, https://doi.org/10.1073/pnas.1717312115, http://www.pnas.org/content/early/2018/02/06/1717312115, 2018.

Noël, B., van de Berg, W., Lhermitte, S., Wouters, B., Machguth, H., Howat, I., Citterio, M., Moholdt, G., Lenaerts, J., and van den Broeke, M. R.: A tipping point in refreezing accelerates mass loss of Greenland's glaciers and ice caps, Nature Communications, 8, 14 730, 2017.

Noël, B., van de Berg, W. J., van Wessem, J. M., van Meijgaard, E., van As, D., Lenaerts, J. T. M., Lhermitte, S., Kuipers Munneke, P., Smeets, C. J. P. P., van Ulft, L. H., van de Wal, R. S. W., and van den Broeke, M. R.: Modelling the climate and surface mass balance of polar ice sheets using RACMO2 – Part 1: Greenland (1958–2016), The Cryosphere, 12, 811–831, https://doi.org/10.5194/tc-12-811-2018, https://www.the-cryosphere.net/12/811/2018/, 2018.

Nowicki, S., Bindschadler, R. A., Abe-Ouchi, A., Aschwanden, A., Bueler, E., Choi, H., Fastook, J., Granzow, G., Greve, R., Gutowski, G., Herzfeld, U., Jackson, C., Johnson, J., Khroulev, C., Larour, E., Levermann, A., Lipscomb, W. H., Martin, M. A., Morlighem, M., Parizek, B. R., Pollard, D., Price, S. F., Ren, D., Rignot, E., Saito, F., Sato, T., Seddik, H., Seroussi, H., Takahashi, K., Walker, R., and Wang, W. L.: Insights into spatial sensitivities of ice mass response to environmental change from the SeaRISE ice sheet modeling project II: Greenland, Journal of Geophysical Research: Earth Surface, 118, 1025–1044, https://doi.org/10.1002/jgrf.20076, 2013.

Nowicki, S. M. J., Payne, A., Larour, E., Seroussi, H., Goelzer, H., Lipscomb, W., Gregory, J., Abe-Ouchi, A., and Shepherd, A.: Ice Sheet Model Intercomparison Project (ISMIP6) contribution to CMIP6, Geoscientific Model Development, 9, 4521–4545, https://doi.org/10.5194/gmd-9-4521-2016, 2016.

Oerlemans, J. and Knap, W. H.: A 1 year record of global radiation and albedo in the ablation zone of Morteratschgletscher, Switzerland, Journal of Glaciology, 44, 231–238, https://doi.org/10.3189/S0022143000002574, 1998.

Pattyn, F.: A new three-dimensional higher-order thermomechanical ice sheet model: Basic sensitivity, ice stream development, and ice flow across subglacial lakes, Journal of Geophysical Research: Solid Earth, 108, https://doi.org/10.1029/2002JB002329, https://agupubs.onlinelibrary.wiley.com/doi/abs/10.1029/2002JB002329, 2003.

Pithan, F. and Mauritsen, T.: Arctic amplification dominated by temperature feedbacks in contemporary climate models, Nature Geoscience, 7, 181–184, https://doi.org/10.1038/ngeo2071, https://www.nature.com/articles/ngeo2071, 2014.

Price, S. F., Payne, A. J., Howat, I. M., and Smith, B. E.: Committed sea-level rise for the next century from Greenland ice sheet dynamics during the past decade, Proceedings of the National Academy of Sciences, 108, 8978–8983, https://doi.org/10.1073/pnas.1017313108, 2011.

Rietbroek, R., Brunnabend, S.-E., Kusche, J., Schröter, J., and Dahle, C.: Revisiting the contemporary sea-level budget on global and regional scales, Proceedings of the National Academy of Sciences, 113, 1504–1509, https://doi.org/10.1073/pnas.1519132113, 2016.

Rignot, E. and Mouginot, J.: Ice flow in Greenland for the International Polar Year 2008–2009, Geophysical Research Letters, 39, n/a–n/a, https://doi.org/10.1029/2012GL051634, 2012.

Rogelj, J., Luderer, G., Pietzcker, R. C., Kriegler, E., Schaeffer, M., Krey, V., and Riahi, K.: Energy system transformations for limiting end-of-century warming to below 1.5°C., Nature Clim. Change, 5, 519–527, http://dx.doi.org/10.1038/nclimate2572, 2015.

Seroussi, H., Morlighem, M., Rignot, E., Khazendar, A., Larour, E., and Mouginot, J.: Dependence of century-scale projections of the Greenland ice sheet on its thermal regime, Journal of Glaciology, 59, 1024–1034, https://doi.org/doi:10.3189/2013JoG13J054, 2013.

Seroussi, H., Morlighem, M., Larour, E., Rignot, E., and Khazendar, A.: Hydrostatic grounding line parameterization in ice sheet models, The Cryosphere, 8, 2075–2087, https://doi.org/10.5194/tc-8-2075-2014, 2014.

Shapiro, N. and Ritzwoller, M.: Inferring surface heat flux distributions guided by a global seismic model: Particular application to Antarctica, Earth and Planetary Science Letters, 223, 213–224, https://doi.org/10.1016/j.epsl.2004.04.011, 2004.

UNFCCC: Adoption of the Paris Agreement, Decision 1/CP.21 of FCCC/CP/2015/10/Add.1, available at: http://unfccc.int/resource/docs/2015/cop21/eng/10a01.pdf (last access: April 2018), 2015.

van de Wal, R. S. W.: Mass-balance modelling of the Greenland ice sheet: a comparison of an energy-balance and a degree-day model, Annals of Glaciology, 23, 36–45, https://doi.org/10.3189/S0260305500013239, 1996.

van den Broeke, M. R., Enderlin, E. M., Howat, I. M., Kuipers Munneke, P., Noël, B. P. Y., van de Berg, W. J., van Meijgaard, E., and Wouters, B.: On the recent contribution of the Greenland ice sheet to sea level change, The Cryosphere, 10, 1933–1946, https://doi.org/10.5194/tc-10-1933-2016, 2016.

Vizcaíno, M., Mikolajewicz, U., Jungclaus, J., and Schurgers, G.: Climate modification by future ice sheet changes and consequences for ice sheet mass balance, Climate Dynamics, 34, 301–324, https://doi.org/10.1007/s00382-009-0591-y, 2010.

Watterson, I. G., Bathols, J., and Heady, C.: What Influences the Skill of Climate Models over the Continents?, Bulletin of the American Meteorological Society, 95, 689–700, https://doi.org/10.1175/BAMS-D-12-00136.1, 2014.

Wilson, N., Straneo, F., and Heimbach, P.: Submarine melt rates and mass balance for Greenland's remaining ice tongues, The Cryosphere Discussions, 2017, 1–17, https://doi.org/10.5194/tc-2017-99, 2017.

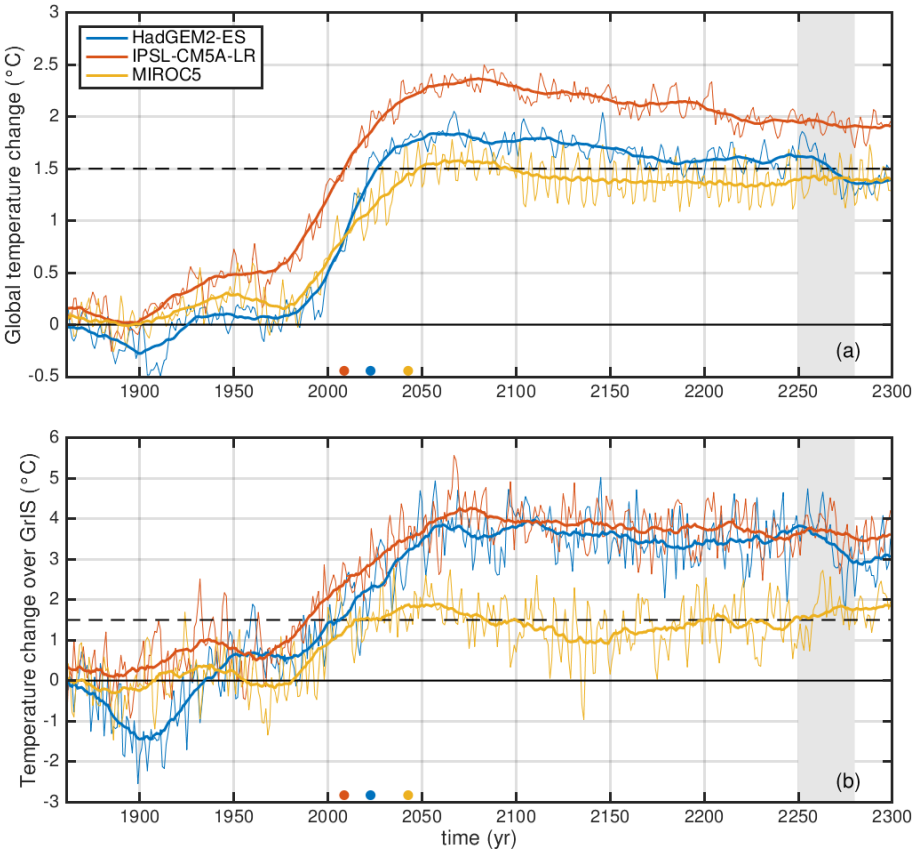

Figure 1. Time series of annual global mean near-surface temperature change (a) and over the GrIS (b) for all three GCMs relative to 1661–1880. The thick line is a 30-year moving mean. The ~~coloured~~ colored dots represent the onset years of overshooting 1.5°C in the global mean near-surface air temperature in a ~~11-year~~ 30-year moving window relative to pre-industrial levels. The light ~~grey~~ gray shaded area indicates the reused time period for the scenario without overshoot.

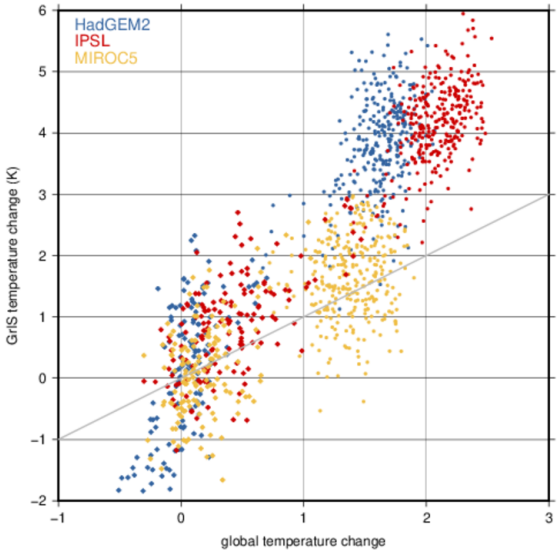

Figure 2. Scatter plot of annual mean near-surface air ~~temperatures~~ temperature change relative to pre-industrial levels over GrIS versus annual global mean near-surface air ~~temperatures~~ temperature change for the years 1861–2299. The ~~grey~~ gray line depicts the identity.

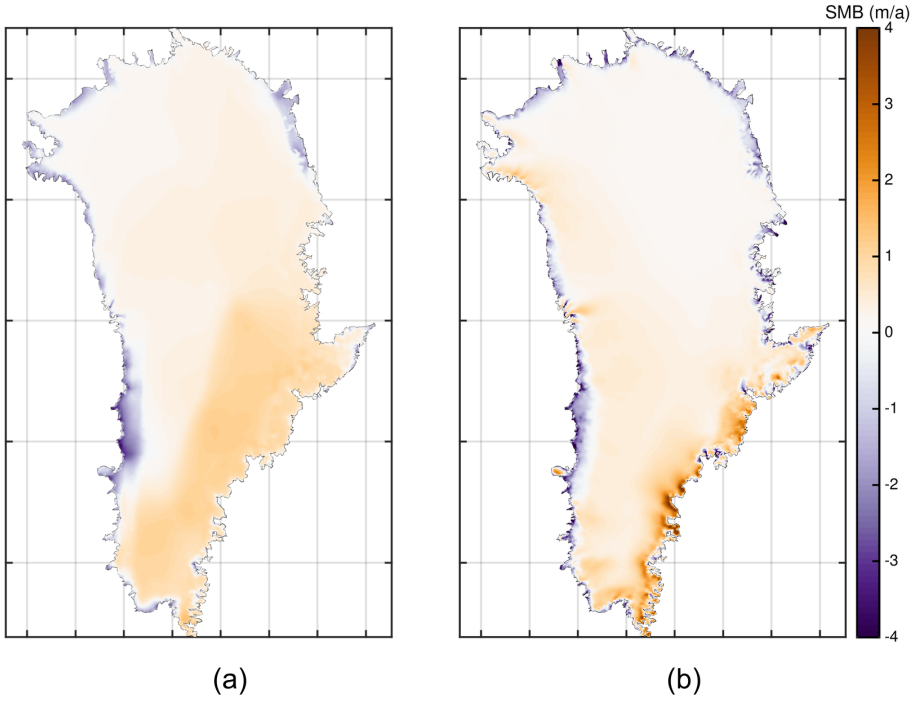

Figure 3. Comparison of surface mass balance fields averaged for the time period 1960–1990; (a) surface mass balance derived by forcing SEMIC with climate data from HadGEM2; (b) surface mass balance of RACMO2.3 (Noël et al., 2018).

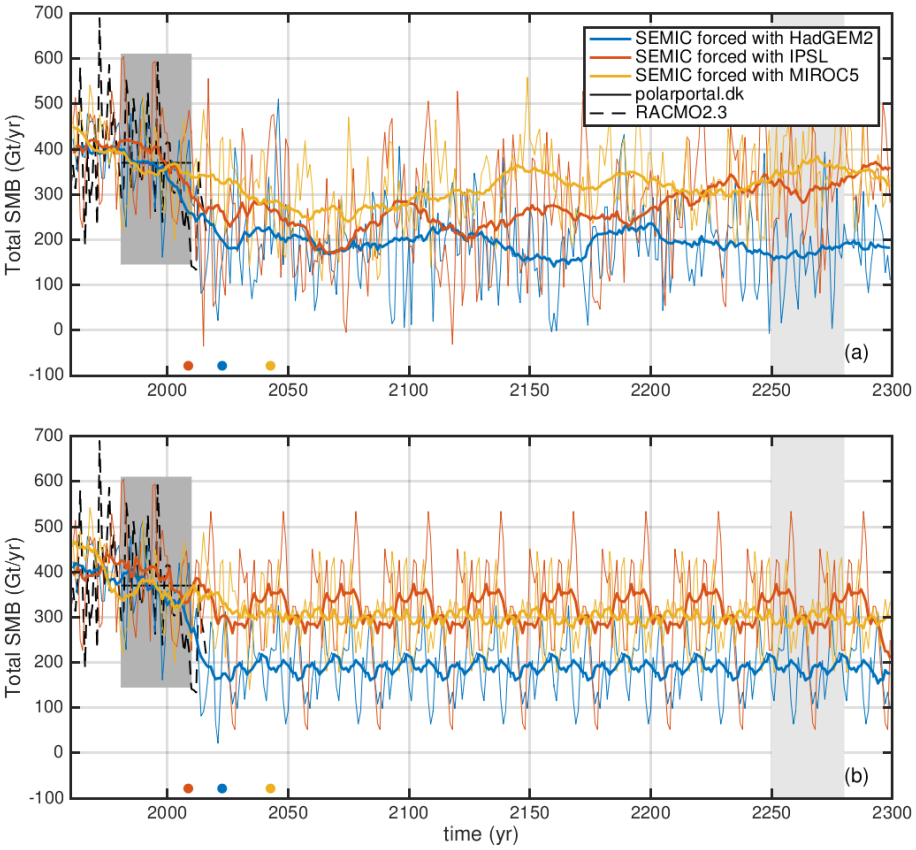

Figure 4. Time series of the annual mean integrated SMB_{clim} ($Gt\,yr^{-1}$) according to Eq.~~3~~ 4 for all three ~~GCMs~~ SEMIC-GCMs under RCP2.6 forcing (a) and RCP2.6 forcing without overshoot (b). The ~~thick~~ solid line is a 30-year and 15-year moving mean in (a) and (b), respectively. In ~~grey~~ gray colour and black line the range and mean of SMB between 1981–2010 from Polarportal is marked (polarportal.dk). The dashed line shows the SMB time series of RACMO2.3 (Noël et al., 2018) from 1958-2016. The ~~coloured~~ colored dots represent the onset years of overshooting 1.5°C in the global mean near-surface air temperature in a ~~11-year~~ 30-year moving window relative to pre-industrial levels. The light ~~grey~~ gray shaded ~~area indicate the reused~~ time period indicates the repeated SMB forcing taken from the RCP2.6 scenario for the scenario without overshoot.

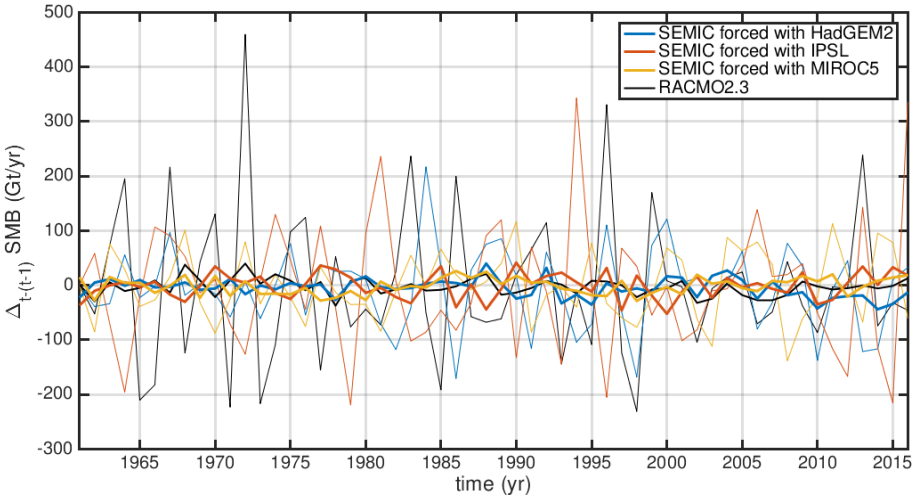

Figure 5. ~~Coefficients of determination r^2~~ Interannual SMB variability for alls SEMIC-GCMs (~~straight~~ colored lines~~and left y-axis~~) and ~~mean singed difference MSD (dashed lines and right y-axis) between the GCM and~~ RACMO2.3 ~~SMB components~~(black line) calculated from consecutive years, $\Delta\text{SMB} = \text{SMB}_t - \text{SMB}_{t-1}$. ~~GCM colour code~~ The solid line is ~~the same as Fig~~is a 30-year moving mean. ~~4.~~

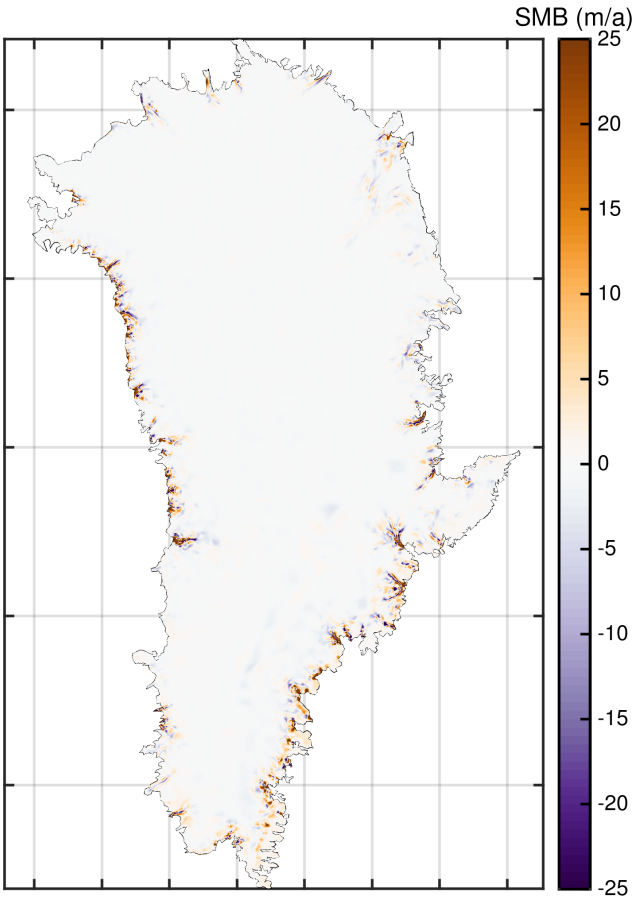

Figure 6. Synthetic surface mass balance SMB_{corr} calculated from an one year unforced relaxation run (truncated at -25 and 25 m a^{-1}). As the SMB_{corr} will be subtracted in Eq. 8 positive values represent enforced thinning; negative values thickening.

~~Comparison of the surface mass balance (SMB_{clim}) for the year 1990; (a) surface mass balance of RACMO2.3 (Noël et al., 2018); (b) surface mass balance for HadGEM2-ES according to Eq. 4; (c) scatter plot of both fields. Positive values represent accumulation (red dots); negative melting (blue dots) with respect to RACMO field.~~

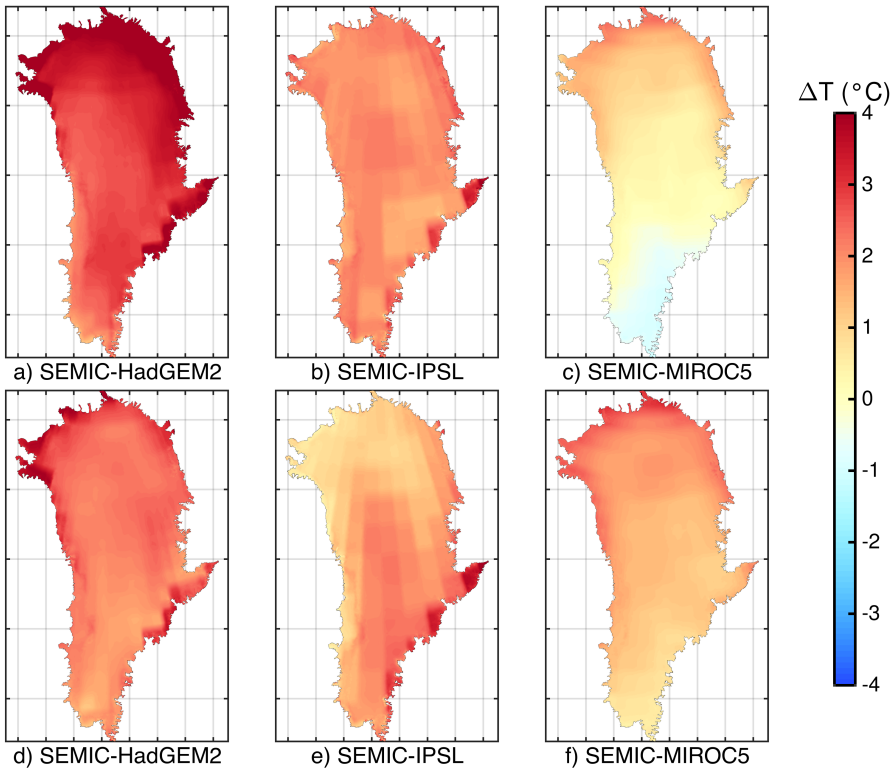

Figure 7. Comparison of multi-year mean surface temperature (T_s) differences between 2100-2000 (top row) and 2300-2000 (bottom row) for (a, d) SEMIC-HadGEM2, (b, e) SEMIC-IPSL and (c, f) SEMIC-MIROC5. The black contour line depicts the present-day ice mask.

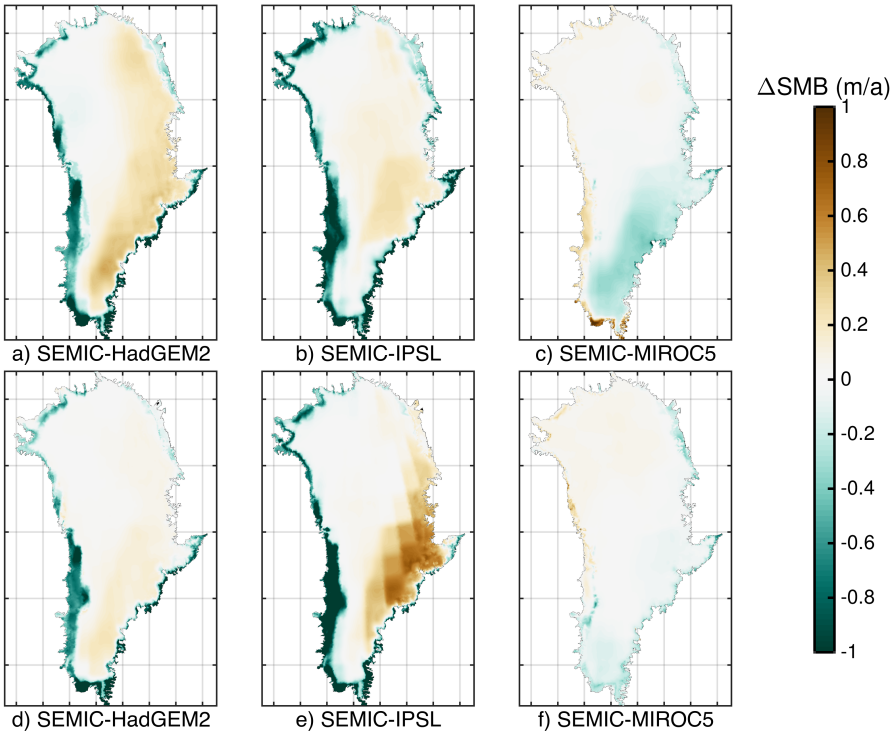

Figure 8. Comparison of multi-year mean surface mass balance (SMB) differences between 2100-2000 (top row) and 2300-2000 (bottom row) for (a, d) SEMIC-HadGEM2, (b, e) SEMIC-IPSL and (c, f) SEMIC-MIROC5. The black contour line depicts the present-day ice mask.

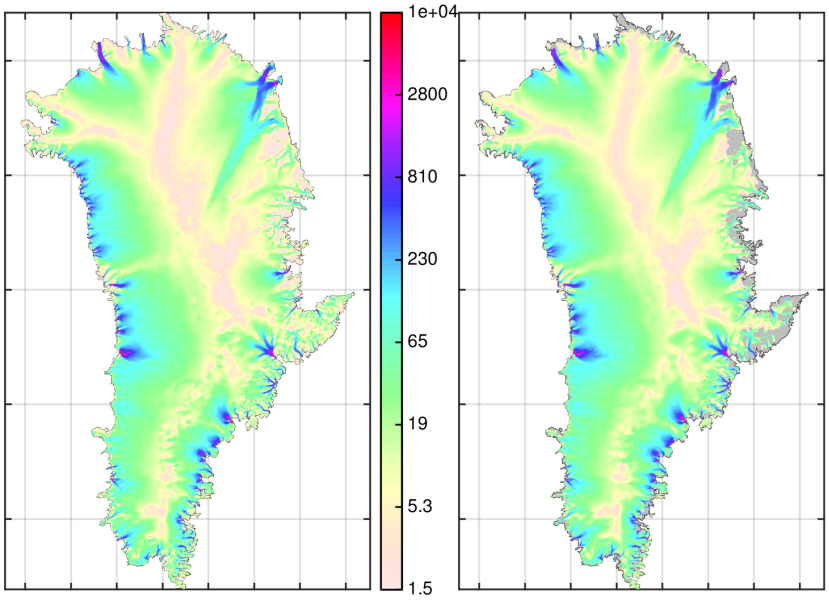

Figure 9. Present day velocities (year 2000) using ~~HadGEM2-ES~~SEMIC-HadGEM2: (a) observed velocities, (b) simulated velocities. Observed velocities: Rignot and Mouginot (2012).

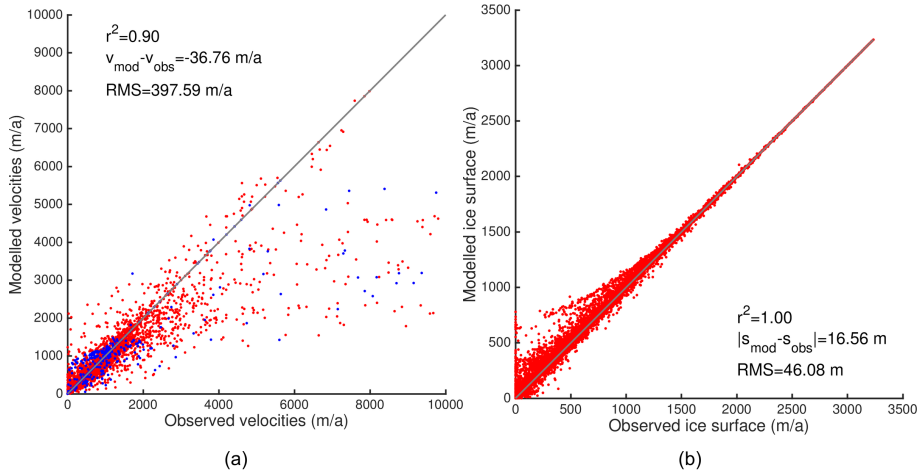

Figure 10. Scatter plots of the present day state (year 2000) using ~~HadGEM2-ES~~the SMB forcing SEMIC-HadGEM2: (a) velocities, (b) ice surface elevation. Blue and red dots in (a) represent floating and grounded points, respectively. Observed velocities: Rignot and Mouginot (2012); Observed surface elevation: Morlighem et al. (2014). The gray line depicts the identity.

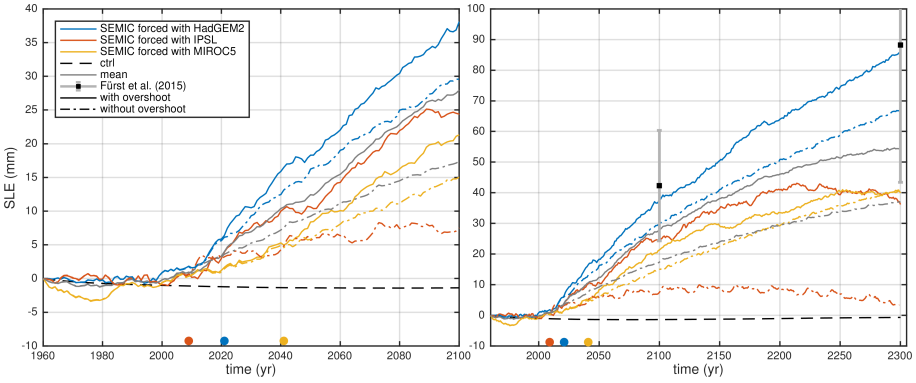

Figure 11. Sea level equivalent (SLE in mm) until the year 2100 (left panel) and 2300 (right panel) ~~for all GCMs. Straight~~ under RCP2.6 forcing (Solid lines~~represent scenario with overshoot; dotted-dashed line~~) and RCP2.6 forcing without overshoot (dotted-dashed). Additionally the control run (black dashed line) and the model mean and rms deviation from Fürst et al. (2015, Table B1) are shown. The ~~coloured~~ colored dots represent the onset years of overshooting 1.5°C in the global mean near-surface air temperature in a ~~11-year~~ 30-year moving window relative to pre-industrial levels.

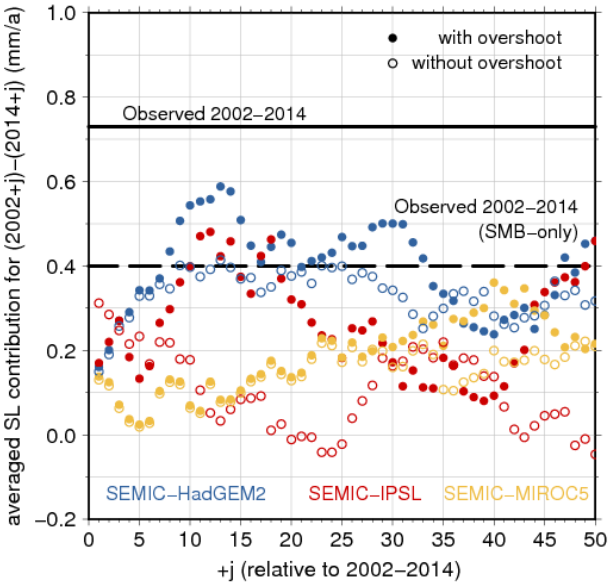

~~Comparison of multi-year mean surface temperature (T_s) differences between 2100-2000 (top row)~~ and ~~2300-2000 (bottom row) for (a, d) HadGEM2-ES, (b, e) IPSL-CM5A-LR and (c, f) MIROC5. The black contour~~ the dashed line ~~depicts~~ the ~~present-day ice mask.~~ ~~Comparison~~ observed value of ~~multi-year mean surface mass balance (SMB) differences between 2100-2000 (top row) and 2300-2000 (bottom row) for (~~0.40 mm a~~, d) HadGEM2-ES, (b, e) IPSL-CM5A-LR and (c, f) MIROC5. The black contour line depicts~~ $^{-1}$ calculated from RACMO2.3 for the ~~present-day ice mask~~period 2002-2014.

~~Comparison of multi-year mean surface temperature (T_s) differences between 2100-2000 (top row)~~ and ~~2300-2000 (bottom row) for (a, d) HadGEM2-ES, (b, e) IPSL-CM5A-LR and (c, f) MIROC5. The black contour~~ the dashed line ~~depicts~~ the ~~present-day ice mask.~~

~~Comparison~~ observed value of ~~multi-year mean surface mass balance (SMB) differences between 2100-2000 (top row) and 2300-2000 (bottom row) for (~~0.40 mm a~~, d) HadGEM2-ES, (b, e) IPSL-CM5A-LR and (c, f) MIROC5. The black contour line depicts~~ $^{-1}$ calculated from RACMO2.3 for the ~~present-day ice mask~~period 2002-2014.

Figure 12. Lag (j) of projected sea level rise per year ~~for three GCMs~~ under RCP2.6 forcing (colored dots) and the modified RCP2.6 forcing without overshoot (colored circles) as mean for a time period similar to the observational period (~~2002–14~~2002–2014). The black line indicates the observed value of 0.73 mm a^{-1} by Rietbroek et al. (2016) ~~.~~

~~Comparison of multi-year mean surface temperature (T_s) differences between 2100-2000 (top row)~~ and ~~2300-2000 (bottom row) for (a, d) HadGEM2-ES, (b, e) IPSL-CM5A-LR and (c, f) MIROC5. The black contour~~ the dashed line ~~depicts~~ the ~~present-day ice mask.~~

~~Comparison~~ observed value of ~~multi-year mean surface mass balance (SMB) differences between 2100-2000 (top row) and 2300-2000 (bottom row) for (~~0.40 mm a~~, d) HadGEM2-ES, (b, e) IPSL-CM5A-LR and (c, f) MIROC5. The black contour line depicts~~ $^{-1}$ calculated from RACMO2.3 for the ~~present-day ice mask~~period 2002-2014.

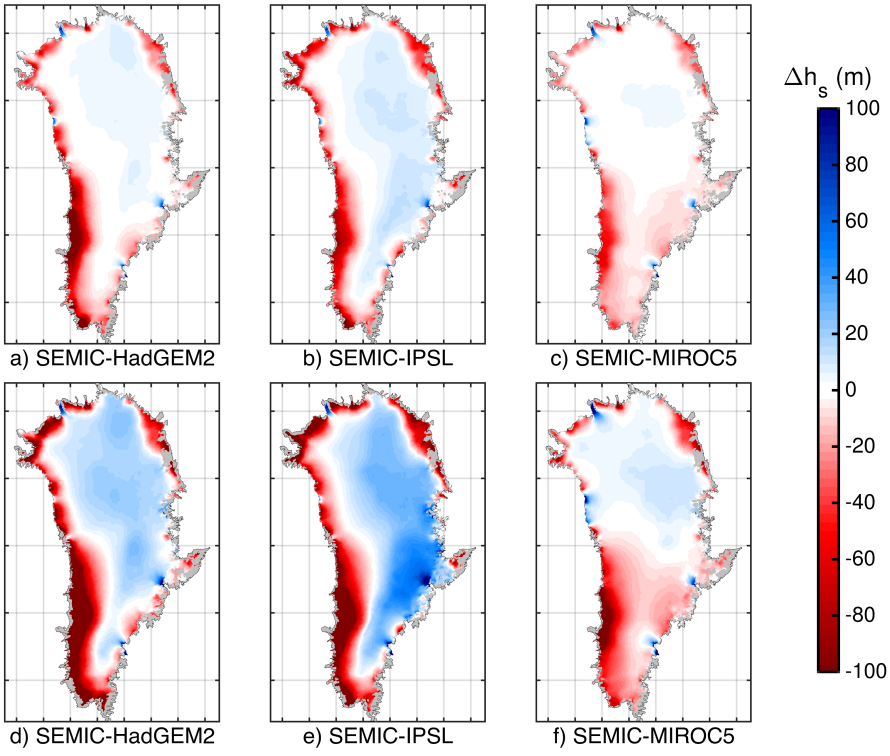

Figure 13. Comparison of multi-year mean surface elevation (h_s) differences under RCP2.6 forcing between 2100-2000 (top row) and 2300-2000 (bottom row) for (a, d) ~~HadGEM2-ES~~SEMIC-HadGEM2, (b, e) ~~IPSL-CM5A-LR~~ SEMIC-IPSL and (c, f) ~~MIROC5~~SEMIC-MIROC5. The black contour line depicts the present-day ice mask. Positive values represent glacier thinning; negative values ~~thickenning~~thickening. The data are clipped at ice thickness of 10 m (~~grey~~ gray shaded area).

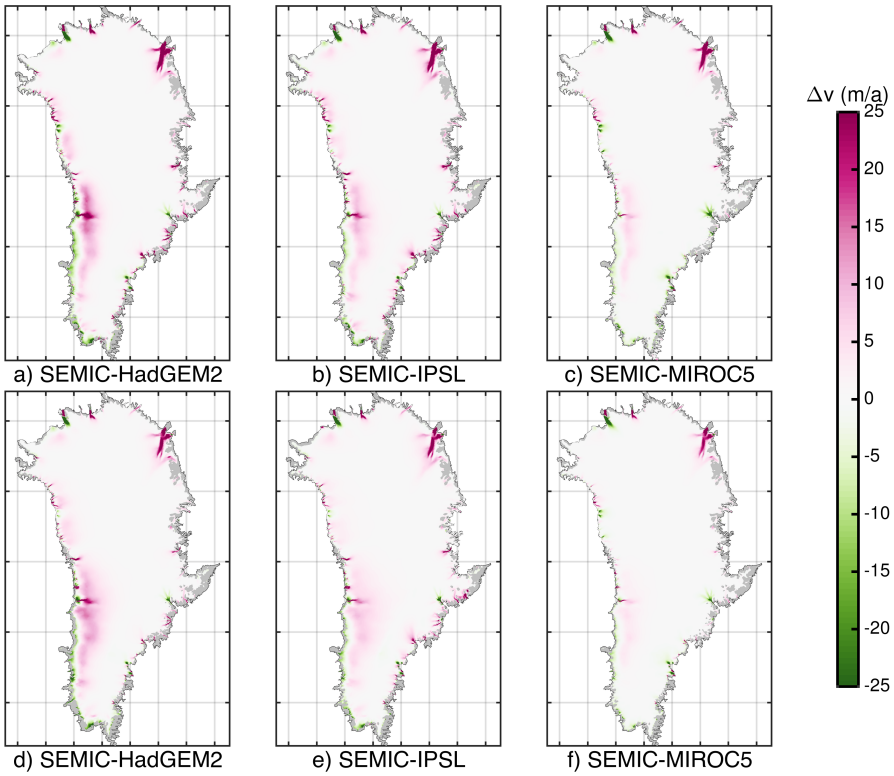

Figure 14. Comparison of multi-year mean surface velocity (v) differences under RCP2.6 forcing between 2100-2000 (top row) and 2300-2000 (bottom row) for (a, d) ~~HadGEM2-ES~~SEMIC-HadGEM2, (b, e) ~~IPSL-CM5A-LR~~ SEMIC-IPSL and (c, f) ~~MIROC5~~SEMIC-MIROC5. The black contour line depicts the present-day ice mask. Positive values represent glacier acceleration; negative values deceleration. The data are clipped at ice thickness of 10 m (~~grey~~ gray shaded area).